NAVAL POSTGRADUATE SCHOOL

MONTEREY, CALIFORNIA

THESIS

THE LARGE-SCALE ENVIRONMENT DURING THE TROPICAL CYCLONE STRUCTURE 2008 AND THORPEX PACIFIC ASIAN REGIONAL CAMPAIGN

by

Ricardo A. Trevino

March 2009

Thesis Advisor: Patrick Harr
Second Reader: Russell Elsberry

Approved for public release; distribution is unlimited.

THIS PAGE INTENTIONALLY LEFT BLANK

1. AGENCY USE ONLY *(Leave blank)*	**2. REPORT DATE** March 2009	**3. REPORT TYPE AND DATES COVERED** Master's Thesis	
4. TITLE AND SUBTITLE The Large-Scale Environment during the Tropical Cyclone Structure 2008 and THORPEX Pacific Asian Regional Campaign		**5. FUNDING NUMBERS**	
6. AUTHOR(S) Ricardo A. Trevino			
7. PERFORMING ORGANIZATION NAME(S) AND ADDRESS(ES) Naval Postgraduate School Monterey, CA 93943-5000		**8. PERFORMING ORGANIZATION REPORT NUMBER**	
9. SPONSORING /MONITORING AGENCY NAME(S) AND ADDRESS(ES) N/A		**10. SPONSORING/MONITORING AGENCY REPORT NUMBER**	
11. SUPPLEMENTARY NOTES The views expressed in this thesis are those of the author and do not reflect the official policy or position of the Department of Defense or the U.S. Government.			
12a. DISTRIBUTION / AVAILABILITY STATEMENT Approved for public release; distribution is unlimited.		**12b. DISTRIBUTION CODE**	

13. ABSTRACT (maximum 200 words)

     This study examines the effects of large-scale circulations (e.g., ENSO, Pacific Decadal Oscillation (PDO), Indian Ocean Dipole (IOD), Antarctic Oscillation (AAO), and Monsoon Trough (MT)) on tropical cyclone (TC) activity in the Western North Pacific (WNP) during the May through October timeframe from 1979 to 2008. The specific objective is to understand how these circulations affected the THORPEX/T-PARC/TCS-08 experiments held during August to October 2008.

     Pivot tables and t-tests were used to analyze the effects of combinations of these circulations on TC activity. Composites of OLR and 850- and 200-hPa winds were constructed to emphasize significant differences between phases of large-scale circulations and combinations. Differences between opposing phases were also analyzed.

     A statistically-significant relationship exists between ENSO phase and TC activity in terms of Accumulated Cyclone Energy (ACE) values and super-typhoon (STY) numbers. The relationship is less significant, but substantial, for the PDO signal analyzed. However, IOD and AAO have even less significance. The MT signal is significant in the ACE values, but less significant in the STY numbers. The conclusions were that ENSO strongly moderates TC activity and numbers of the most intense TCs in the WNP, while PDO, IOD, and AAO merely reinforce a positive or negative phase of the ENSO circulations. The MT signal has significance on TC activity, but little effect on STY numbers.

14. SUBJECT TERMS Large-Scale Tropical Circulations, Tropical Cyclones, ENSO, Pacific Decadal Oscillation, Indian Ocean Dipole, Antarctic Oscillation, Monsoon Trough, Interannual Variability			**15. NUMBER OF PAGES** 87
			16. PRICE CODE
17. SECURITY CLASSIFICATION OF REPORT Unclassified	**18. SECURITY CLASSIFICATION OF THIS PAGE** Unclassified	**19. SECURITY CLASSIFICATION OF ABSTRACT** Unclassified	**20. LIMITATION OF ABSTRACT** UU

THIS PAGE INTENTIONALLY LEFT BLANK

THE LARGE-SCALE ENVIRONMENT DURING THE TROPICAL CYCLONE STRUCTURE 2008 AND THORPEX PACIFIC ASIAN REGIONAL CAMPAIGN

Ricardo A. Trevino
Lieutenant Commander, United States Navy
B.A., University of North Florida, 2000

Submitted in partial fulfillment of the
requirements for the degree of

MASTER OF SCIENCE IN METEOROLOGY AND OCEANOGRAPHY

from the

NAVAL POSTGRADUATE SCHOOL
March 2009

Author: Ricardo A. Trevino

Approved by: Patrick Harr
                      Thesis Advisor

                      Russell Elsberry
                      Second Reader

                      Philip Durkee
                      Chairman, Department of Meteorology

THIS PAGE INTENTIONALLY LEFT BLANK

ABSTRACT

This study examines the effects of large-scale circulations (e.g., ENSO, Pacific Decadal Oscillation (PDO), Indian Ocean Dipole (IOD), Antarctic Oscillation (AAO), and Monsoon Trough (MT)) on tropical cyclone (TC) activity in the Western North Pacific (WNP) during the May through October timeframe from 1979 to 2008. The specific objective is to understand how these circulations affected the THORPEX/T-PARC/TCS-08 experiments held during August to October 2008.

Pivot tables and t-tests were used to analyze the effects of combinations of these circulations on TC activity. Composites of OLR and 850- and 200-hPa winds were constructed to emphasize significant differences between phases of large-scale circulations and combinations. Differences between opposing phases were also analyzed.

A statistically significant relationship exists between ENSO phase and TC activity in terms of Accumulated Cyclone Energy (ACE) values and super-typhoon (STY) numbers. The relationship is less significant, but substantial, for the PDO signal analyzed. However, IOD and AAO have even less significance. The MT signal is significant in the ACE values, but less significant in the STY numbers. The conclusions were that ENSO strongly moderates TC activity and numbers of the most intense TCs in the WNP, while PDO, IOD, and AAO merely reinforce a positive or negative phase of the ENSO circulations. The MT signal has significance on TC activity, but little effect on STY numbers.

THIS PAGE INTENTIONALLY LEFT BLANK

TABLE OF CONTENTS

THIS PAGE INTENTIONALLY LEFT BLANK

LIST OF FIGURES

THIS PAGE INTENTIONALLY LEFT BLANK

LIST OF TABLES

THIS PAGE INTENTIONALLY LEFT BLANK

ACKNOWLEDGMENTS

THIS PAGE INTENTIONALLY LEFT BLANK

I. INTRODUCTION

A. OBJECTIVE

Tropical cyclones (TCs) can be a devastating and particularly powerful form of weather that, by its inherent nature, can cause significant destruction, immense financial disruption, and great loss of life. Also distressing is the prospect of TCs disrupting important lines of military operations, lines of communications, and/or logistics (i.e., resources, fuel, supplies, etc.) during peace and wartime operations. The U.S. Navy has invested a great deal of time, effort, and money in the research and forecasting of TC genesis, motion, and intensification. Many experiments have been devoted to studying TC formation, track, and intensity. The long-range forecasting of TC activity has become more important to naval operations and interests. Often, climatology and statistical methods are used to identify seasons that may be more active than others based on large- and small-scale environmental factors. Knowing where a TC will form, when it will form, and what intensity it will reach has been an inexact science that has perplexed forecasters for many years. However, the advent of satellite meteorology, increased amounts of data in certain areas, supercomputers, etc., have been able to improve forecasts of TC characteristics. Additionally, new techniques and identification of important large-scale atmospheric characteristics are providing increased awareness as to how active a particular season will be and where TCs can be expected. The military will continue to benefit from these studies and the ability to plan for forecasts of such destructive events, as they may affect operational factors (space, time, and force) and operational functions.

Chan et al. (1998) found that TC activity over the western North Pacific (WNP) involves variations on timescales of a few years to decades. Since these variations have certain identifiable periods, Chan et al. hypothesized that it may be possible to develop a statistical forecasting tool to predict the TC activity for a particular season, the same way it has been successfully done for the Atlantic basin since 1989 by other scientists (e.g., Gray et al. 1989). Various statistical forecasting aids have been defined that include

predictors related to the El Niño (EN)/Southern Oscillation (ENSO), strength of the Australian monsoon, and intensity of the subtropical high in the South Pacific. In general, these efforts have resulted in better forecasts of seasonal TC activity (Chan et al. 2001).

Delk (2004) studied large-scale circulations that force sub-monthly periods of enhanced and reduced convection over the WNP and their effects on TC activity. Delk further described the effects of the large-scale basic state on the occurrence and structure of the primary tropical synoptic-scale disturbances over the region, and how the basic state may be influenced by several slowly-varying, global-scale circulation systems. Using singular value decomposition (SVD), Delk identified a Northern Hemisphere (NH) 15- to 25-day oscillation that modulates TC genesis in the WNP monsoon trough (MT) region on weekly timescales. Delk concluded that a statistically significant relationship exists between the 15- to 25-day cycle and TC occurrence in the WNP, and that this cycle not only impacts the numbers of cyclones formed, but also the formation locations.

Burton (2005) examined the characteristics of Southern Hemisphere (SH) wave activity over the mid-latitudes that appeared to have a connection to the 15- to 25-day wave activity in the WNP MT. Using empirical orthogonal function (EOF) analysis, composites, temporal analysis, and single event analysis, Burton investigated the role of the SH Annular Mode in modulating intraseasonal wave activity in the WNP, and potential impacts on the 15- to 25- day oscillation. He concluded that nearly one half of the significant 15- to 25-day MT variations coincide with a transition of the Antarctic Oscillation (AAO) from a significant negative to positive index. According to Burton, identification of 15- to 25-day variability together with AAO activity could help identify periods of MT variability on intraseasonal scales.

While factors such as those identified above influence TC activity on intraseasonal scales, interannual variability is due to other global-scale circulation modes. Because of the highly anomalous 2008 TC season over the WNP, the objective of this thesis is to understand influences of large-scale circulations, such as the Pacific Decadal Oscillation (PDO), ENSO, the AAO, the Indian Ocean Dipole (IOD), and the Monsoon Trough (MT) on TC activity in the WNP on seasonal time scales.

The focus will be on the most predominant large-scale circulations, while only briefly examining the effects of smaller-scale/regional circulation features (i.e., Kelvin Waves, Equatorial Rossby Waves, Mixed Rossby-Gravity Waves, tropical waves, etc.). According to Frank and Roundy (2006), large-scale tropical waves are known to have an impact on tropical weather patterns and enhance local circulations by "increasing the forced upward vertical motion, increasing the low-level vorticity at the genesis location, and by modulating the vertical shear." They further state "tropical cyclones form in regions of preexisting deep, precipitating convection." They ask an important question in their research: "Do the cyclones form quasi randomly from fortuitous interactions between mesoscale convective systems, or do predictable large-scale circulations determine the time and place of genesis?"

B.   MOTIVATION

Among all ocean basins where TCs occur, the WNP has had the largest number of TCs every year except 2005 (Chan 2008). During August to October 2008, the THORPEX (THe Observing system Research and Predictability EXperiment) Pacific Asian Regional Campaign (T-PARC) and Tropical Cyclone Structure 2008 (TCS-08) experiments were conducted to collect observations of the formation, development, movement, intensity, and eventual extratropical transition of a TC. The WNP region was the test bed for these experiments since TC activity is greatest in this period. However, the August –September 2008 period was one of the least active TC periods during recent years and was affected by a variety of anomalous large-scale circulations. Based on preliminary data from the Regional Specialized Meteorological Center (RSMC) — Tokyo (Figure 1), the 2008 season had a total of 22 TCs with two that reached super typhoon (STY) (sustained winds $\geq$ 130 kt) intensity, eight reached typhoon (TY) intensity, eight reached tropical storm (TS) intensity, and three reached only a tropical depression (TD) stage. The total number of TCs in 2008 (Figures 1 and 2) was well below the 30-year-average value of 26.7 (Sasaki 2009). Even though May 2008 was very active with four TCs (two TYs and one STY) while the median for this month is only one, the number of TCs during 2008 was below the long-term average number of storms.

No typhoons occurred during October 2008, which was the first October with no typhoons in the JTWC records that began in 1951. From June to October, 13 TCs occurred and the average is 18.5 (Figure 2). This was the second lowest value recorded (Sasaki 2009) with only 1998 containing fewer (11) TCs (Figure 2). Figure 3 is similar to Figure 2, except for the accumulated cyclone energy (ACE), which is defined as the summation of the 6-hour maximum wind speed squared for the entire season. Only June and September had ACE values nearly equal to the 1979-2008 climatology values. Whereas May had excessive values (owing to the three typhoons), July, August, and October (especially) all had below-climatological ACE values. The anomalous high number of TCs in May resulted in a large ACE value that was also much above normal. During the primary portion of the TC season, only September contained average ACE values, which was due to the occurrence of several long-lived TCs. Every other month contained extremely low values of ACE compared to climatology.
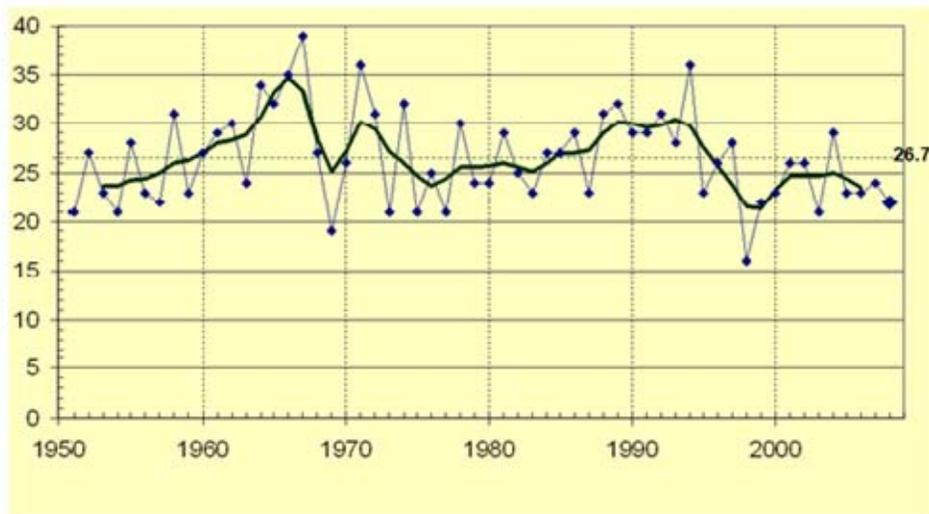
Figure 1.   Annual frequency of named TCs (1951 – 2008) (From: Summary of the 2008 typhoon season by the RSMC Tokyo – Typhoon Center)

4
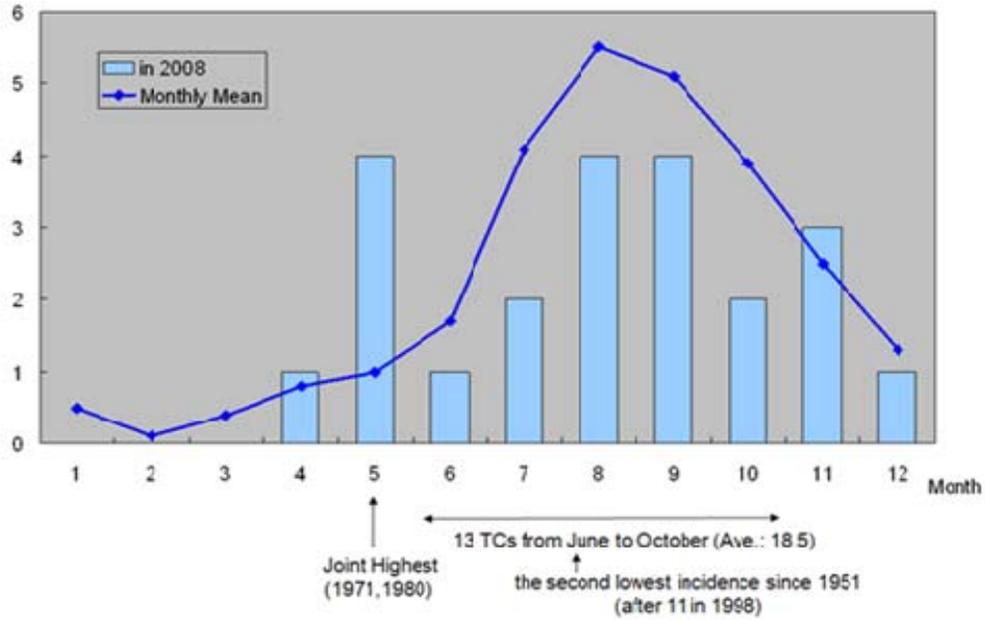
Figure 2.   Monthly frequency of named TCs (tropical storms and typhoons) over the western North Pacific during 2008 (bars) and climatology (line) (From: Summary of the 2008 typhoon season by the RSMC Tokyo – Typhoon Center).
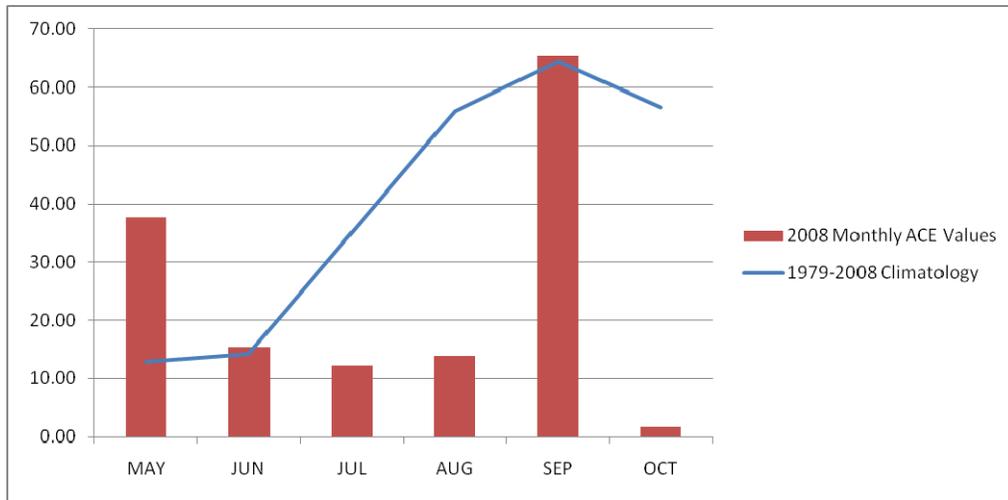
Figure 3.   Monthly ACE values for 2008 (red bars) over the western North Pacific versus the climatology (line). (From: ACE data provided by Suzana Camargo)

The vast majority of storms in 2008 formed west of 140°E (Figure 4) in the Philippine Sea and the South China Sea (SCS), especially as more than the normal number of named TCs occurred west of the Philippines in 2008 (Sasaki 2009).

5
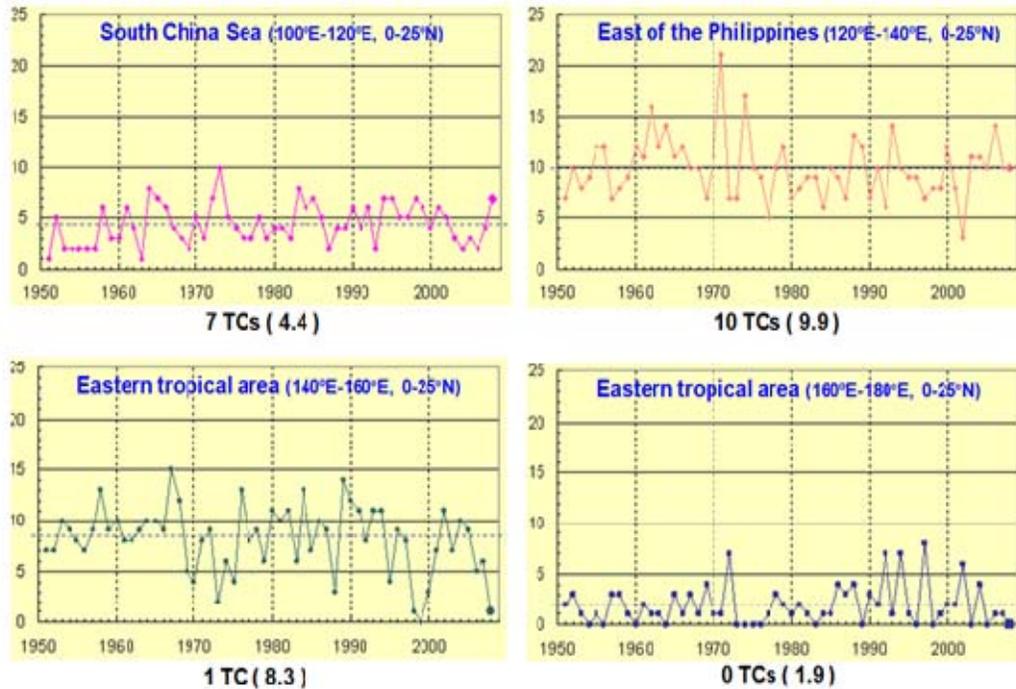
Figure 4.   Annual frequency of named TCs in each area (1951 – 2008) (From: Summary of the 2008 typhoon season by the RSMC Tokyo – Typhoon Center).

Based on a number of official ENSO indices, including the Ocean Niño Index (ONI), 2008 was considered an ENSO-neutral year after coming out of a La Niña (LN) event in May (Figure 5); however, the large-scale atmospheric conditions had many attributes similar to that of a (LN) event. The mean Niño4 Index (Figure 6) from June to November was -0.31. A large area of negative sea-surface temperature (SST) anomalies was found over the subtropical North Pacific east of 170°E. At low levels, easterly wind anomalies occurred over most of the tropical WNP (Figure 7), with a maximum amplitude near 150°E that resulted in a weaker MT. Thus, this area was not favorable for TC genesis (Harr and Elsberry 1991).

Another noteworthy anomalous characteristic of 2008 was an extremely negative phase of the Pacific Decadal Oscillation (PDO), with an average index of -1.565 between May and October, which was one of the lowest PDO values recorded in the last five decades. The PDO is defined (see section I.C.1. below) as an ENSO-like pattern, which shift phases on the order of 20-30 years (versus 6-18 months for ENSO) and has most visible effects in the North Pacific/North American sector and secondary effects over the

tropics (the opposite is true of ENSO). A positive phase is discernible by warm SST anomalies over the eastern Pacific mid-latitudes and a deeper Aleutian Low over the central North Pacific, while a negative phase is indicative of cold SST anomalies near the North American coastline and a stronger anticyclonic anomaly in the central and eastern Pacific mid-latitudes. Thus, positive PDO values are associated with EN-like conditions, while negative PDO values are associated with LN-like conditions.

The combination of these anomalous atmospheric conditions and extremely reduced level of TC activity provides the motivation to examine the relation between these large-scale signals and seasonal TC activity. First, past years with conditions similar to 2008 (i.e., years after a LN event and under the background of a strong negative PDO event) are identified based on the analysis of Chan (2009) (see http://weather.cityu.edu.hk/tc_forecast/2008_Verification.htm for more information). Five such cases are found (Table 1): 1975, 1999, 2000, 2001, and 2008. Four of these five seasons were associated with slightly below- or below-normal TC activity. On the other hand, five TC seasons without a strong negative PDO index (i.e., weak negative or positive index) are associated with above-normal TC activity (Table 1, bottom).
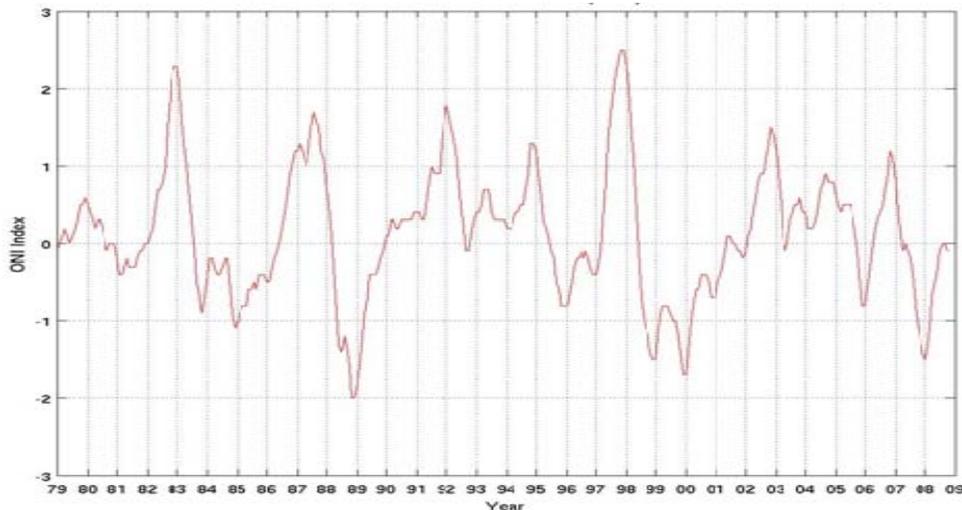
Figure 5. ENSO ONI index from 1979 to October 2008. EN and LN episodes are
defined when the threshold of +/- 0.5°C for ONI is met for a minimum of five
consecutive over-lapping seasons.
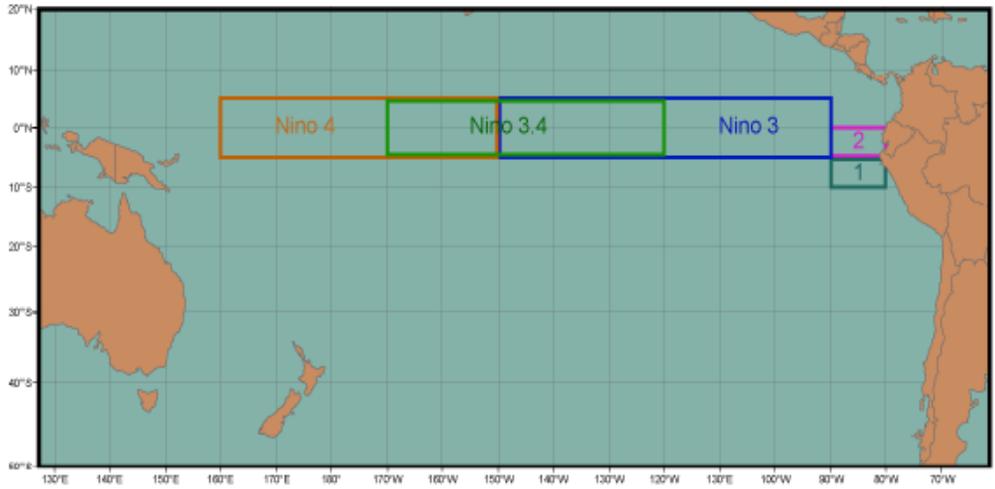
Figure 6.   Nino4 SST Index is averaged in the box 6N-6S, 160E-150W shown above.
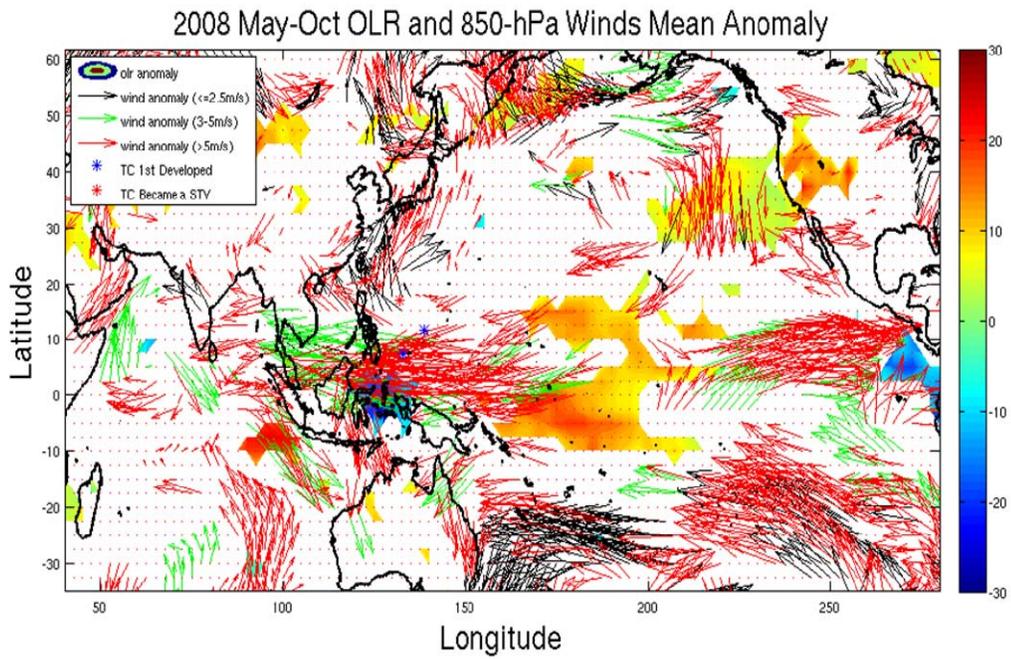
Figure 7.   2008 May-Oct OLR (shaded in W/m^2) and 850 hPa winds (vectors in m/s) anomalies.

Table 1.　　　　Summary of TC activity in the years following La Niña events and (top) associated with a strongly negative PDO index and (bottom) having a weakly negative or positive PDO index. Blue and red shadings indicate the below-normal and above-normal TC activity respectively (From: Verification of forecasts of tropical cyclone activity over the western North Pacific in 2008: http://weather.cityu.edu.hk/tc_forecast/2008_Verification.htm).

	PDO (Jul-Oct)	Niño3.4 (Jul-Oct)	No. of storms and typhoons	No. of typhoons	ENSO status
Years with strong negative PDO					
2008	-1.67	-0.05	25	12	Neutral
1999	-1.35	-0.94	24	12	La Niña
2001	-1.21	0.08	29	20	Neutral
2000	-1.10	-0.42	25	15	La Niña
1975	-1.00	-1.24	20	14	La Niña
Others years					
1971	-0.59	-0.58	35	24	La Niña
1972	-0.08	1.38	30	22	El Niño
1965	-0.01	1.34	34	21	El Niño
1974	0.13	-0.49	32	15	La Niña
1996	0.14	-0.20	33	21	Neutral
1989	0.21	-0.36	31	21	Neutral
1985	0.65	-0.35	26	17	Neutral
1976	0.96	0.51	25	14	El Niño
			Normal: 27	Normal: 17	

C.　　BACKGROUND

Mantua (1999) wrote that, "While the vagaries of climate have often seemed random and unpredictable, recent advances in climate science point to a handful of regularly occurring patterns that impose at least a bit of order in the always variable climate system." It has become clear that many large-scale circulation patterns have distinctive signatures in the seasonally changing regimes of upper- and lower-level winds, air temperature, Outgoing Long-wave Radiation (OLR), convection, and precipitation. Furthermore, each large-scale circulation also has a distinct life cycle and temporal/spatial signature.

Numerous factors (e.g., observational deficiencies over the tropical oceans, inadequate numerical model resolution, and physical process representations) make it difficult to accurately predict the details of the dynamical and thermodynamic processes involved with TC formation. However, there is a tendency for TC activity to cluster in time, which suggests that large-scale environmental factors play some role. In this study, the following large-scale circulation patterns are investigated for their impact on TC activity over the WNP.

1.   Pacific Decadal Oscillation

The PDO is a long-lived El Niño-like pattern of Pacific climate variability (Zhang et al. 1997). However, one temporal and one spatial characteristic distinguish the PDO from the ENSO signal. First, the PDO signal shifts phases (i.e., from warm and cold) on the order of 20-30 years, while ENSO events phase shifts are on the order of 6 to 18 months. Second, the climatic signatures of the PDO are most visible in the North Pacific/North American sector, with secondary signatures over the tropics, which is opposite to ENSO (Mantua et al. 1997; Minobe 1997).

The PDO index is calculated from monthly patterns of North Pacific SST and sea-level pressure (SLP) anomalies, projected onto characteristic SST and SLP patterns, based on a long-term average (Trenberth 1990; Trenberth and Hurrell 1994; Mantua et al. 1997). When SSTs are anomalously low in the interior North Pacific and high along the Pacific coast of North America and when SLP is below-average over the North Pacific (more intense Aleutian Low), the PDO index has positive values (Figure 8 left panel). When the climate anomaly patterns are reversed, with warm SST anomalies in the interior and cool SST anomalies along the North American coast, and above-average SLP over the North Pacific, the index is negative (Figure 8 right panel). Warm phases of the PDO are correlated with EN weather patterns, while cool phases of the PDO are correlated with the reverse climate anomaly patterns, which are broadly similar to typical LN climate patterns (Mantua 1999).
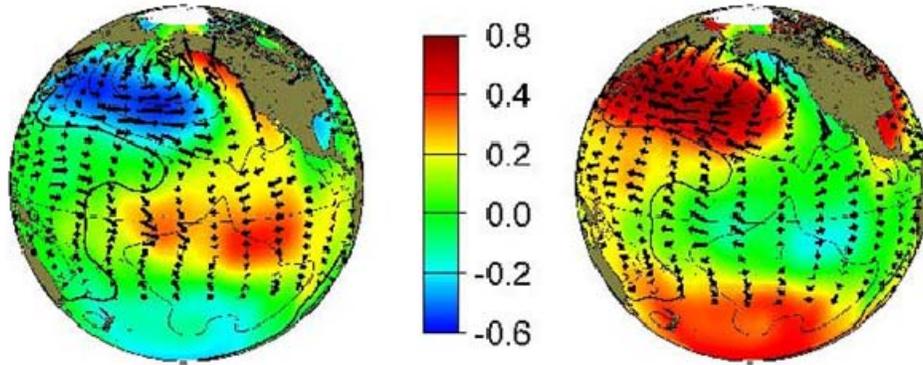
Figure 8.   Schematic of the typical wintertime SST (colors), SLP (contours) and surface wind stress (arrows) anomaly patterns during warm (left panel) and cool (right panel) phases of the PDO (From: http://jisao.washington.edu/pdo/).

Over the past century (Figure 9), the amplitude of the PDO has varied on interannual-to-interdecadal timescales (Mantua et al. 1997). From 1979 to 2008, the PDO has been predominately positive with a few negative episodes. Since September 2007, the PDO has shown a basin-wide cool phase with a 2008 minimum value of -1.76 in October of 2008 (Figure 10). The SST anomalies from 14-21 April 2008 (Figure 11) depict the LN and PDO negative patterns of anomalies in the Pacific Ocean.
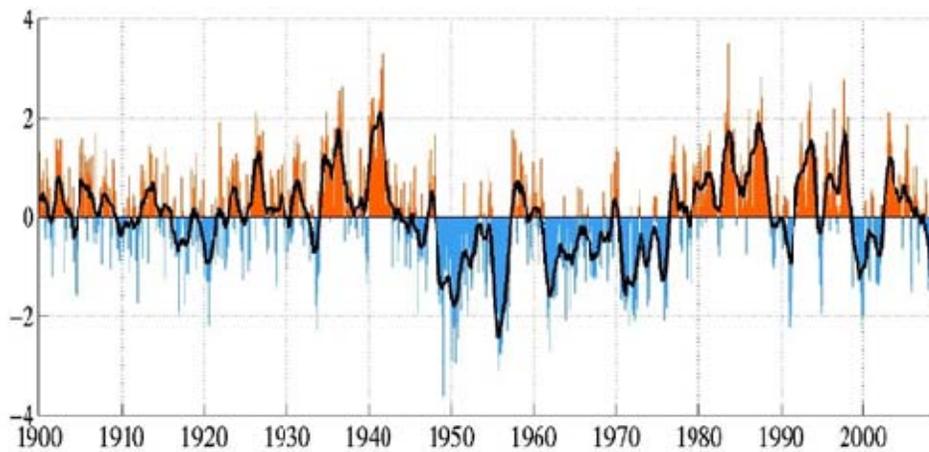
Figure 9.   Monthly values for the PDO index during 1900 to September 2008. The PDO Index is defined as the leading principal component of North Pacific monthly SST variability poleward of 20N during the 1900-93 period (From: http://jisao.washington.edu/pdo/).

11
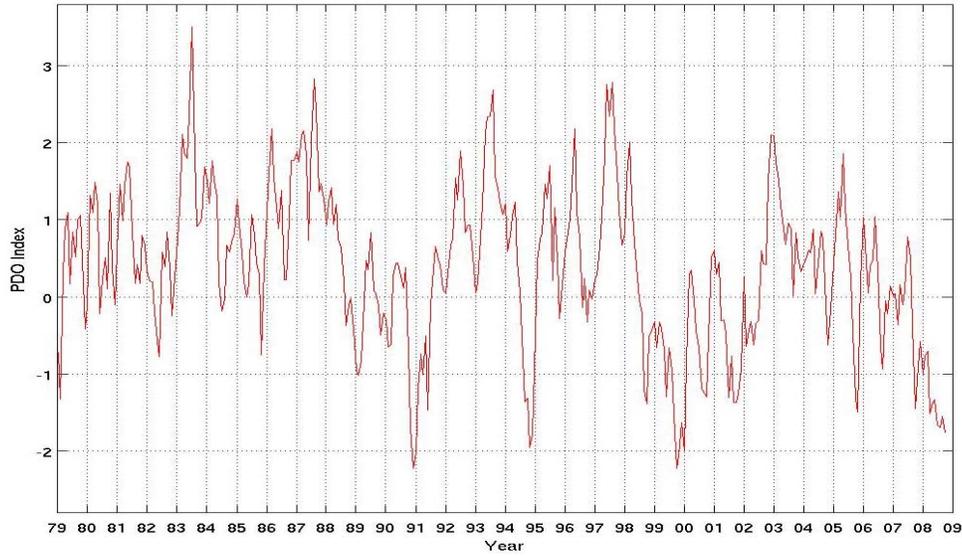
Figure 10.   As in Figure 9, except for years 1979 – October 2008. Above- (below-) normal events are defined by being higher (lower) than one standard deviation ($\sigma_{PDO} = 1.078$).
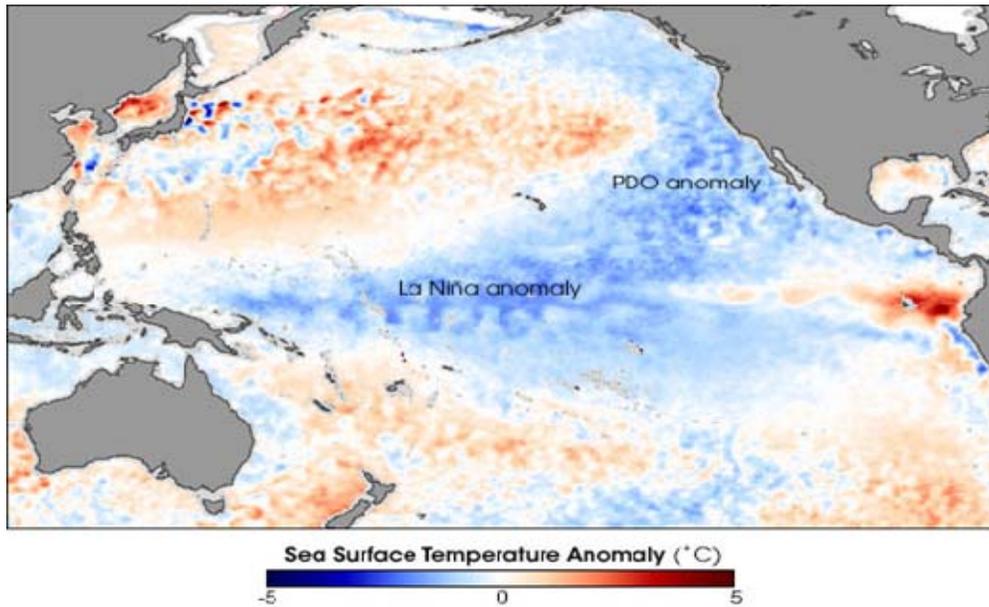
Figure 11.   Sea-surface temperature anomalies from 14-21 April 2008 measured by the Advanced Microwave Scanning Radiometer for EOS (AMSR-E) on the NASA Aqua satellite and computed relative to an average of data collected by the NOAA Pathfinder satellites from 1985–1997 (From: http://jisao.washington.edu/pdo/).

Recent studies (Gershunov and Barnett 1999; Gershunov et al. 2000; McCabe and Dettinger 2002) suggest that ENSO teleconnections with North American climate are strongly dependent on the phase of the PDO, such that the well-defined EN and LN patterns are only valid during years in which ENSO and PDO extremes are "in phase" (i.e., with warm PDO+EN, and cool PDO+LN, but not with other combinations). Therefore, it is likely that a negative PDO can intensify LN or diminish EN impacts in and around the Pacific basin.

Chan (2008) used wavelet analysis to identify two major oscillation periods of 2-7 years and 16-32 years related to the frequency of intense typhoons (categories 4 and 5 in the Saffir-Simpson scale) during 1960-2005. Chan concluded that the frequency of intense typhoons undergoes a strong multi-decadal (16-32 years) variation due to similar variations in the planetary-scale oceanographic and atmospheric conditions that govern the formation, intensification, and movement of TCs. These latter variations are largely contributed by the EN and the PDO on similar time scales. The linear regression correlation coefficient of 0.89 of the ENSO and PDO indices with the number of Category 4 and 5 typhoons means that 79% of the interdecadal variance in intense typhoon activity can be explained by the decadal combined signal of ENSO and PDO. Thus, it is concluded from this result that decadal variations in intense typhoon activity largely result from a combination of the behavior of ENSO and PDO on similar time scales.

2.   El Niño / La Niña Southern Oscillation

The ENSO phenomenon is a global coupled ocean-atmosphere phenomenon that is reflected in the Pacific Ocean as significant fluctuations in SST, pressure, winds, convection, and ocean thermocline (Figure 12). It is the most prominent global source of interannual variability (about 2 to 7 years) in weather and climate.

Rasmussen and Carpenter (1982) identified the evolution of warm ENSO events. During October-November prior to an El Niño event (Figure 12b), the equatorial easterly anomalies in the western Pacific are replaced by westerly anomalies, and positive SST anomalies are present in the vicinity of the equator near the dateline. A westward

migration of the eastern equatorial Pacific SST anomaly pattern from the South American coast into the central equatorial Pacific occurs in conjunction with the intensification of westerly wind anomalies along the equator and the development of anomalous northerly flow across the mean position of the Intertropical Convergence Zone (ITCZ). These variations shift southward at this time and are accompanied by a northeastward shift of the South Pacific Convergence Zone (SPCZ). The result is a smaller wedge-shaped dry zone and enhanced precipitation in the eastern and central tropical Pacific. Below-normal precipitation is observed over Indonesia at this time associated with enhanced divergence and a weakened East Asian northeast winter monsoon. On the other hand, La Niña (Figure 12c) is characterized by an increase in the easterly anomalies in the tropics and greater convection/precipitation in the western Pacific, while drier conditions exist in the eastern Pacific.
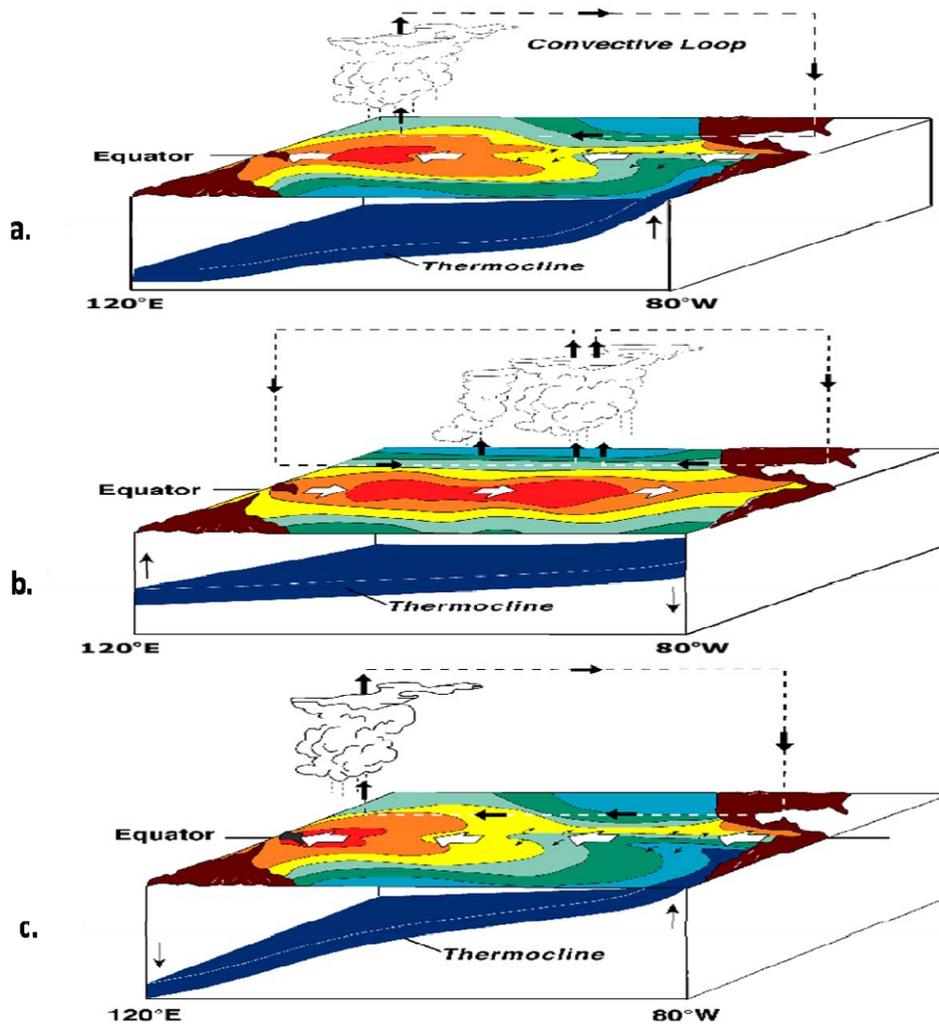
Figure 12.   Three stages of the ENSO: (a) Normal Pacific pattern of equatorial winds, SSTs, and thermocline. (b) El Niño conditions in which warm water approaches the South American coast and an absence of cold upwelling water increases warming along the coast of South America. (c) La Niña conditions in which warm water is located farther west than usual (From: the NOAA Tropical Atmosphere Ocean (TAO) Project: http://www.pmel.noaa.gov/tao/proj_over/diagrams/index.html).

Although various ENSO indices exist, this study utilizes the Ocean Niño Index (ONI, Figure 5) with EN and LN episodes defined when the threshold (+/- 0.5°C) is met for a minimum of five consecutive over-lapping seasons. Comparison of the ONI and PDO index shows that ENSO tends to lead the PDO cycle by approximately 2-6 months in most cases. However, the ENSO of 1991-92 led the (+)PDO by almost 11 months, and the warm phase of 1994 led the (+)PDO by 9 months.

The relationship between the ENSO and WNP TCs has been examined by many authors (see references in Camargo and Sobel 2005). Wang and Chan (2002) analyzed a 35-year (1965-99) record to study the effects of strong ENSO events on tropical storm (TS) activity over the WNP. They concluded that the relationship between the WNP TS activity and ENSO strongly depends on the intensity of ENSO episodes. Whereas strong EN or LN events have significant impacts on the WNP TS activity, the moderate warm/cold events do not show significant impacts. Without distinguishing the impacts between moderate and strong events, one may overestimate the effects of moderate events and underestimate the impacts of the strong events. During EN summer and fall, the frequency of TS formation increases remarkably in the southeast quadrant of the WNP (0°-17°N, 140°E-180°) and decreases in the northwest WNP quadrant (17°-30°N, 120°-140°E). The enhanced TS formation in the SE quadrant is attributed to the increase of the low-level shear vorticity generated by EN-induced equatorial westerlies that extend farther eastward, while the suppressed TS generation over the NW quadrant is ascribed to upper-level convergence induced by the deepening of the east Asian trough and strengthening of the WNP subtropical high, which both result from EN forcing.

Camargo and Sobel (2005) found a positive correlation between the ACE with ENSO indices, and other statistics of warm episodes show that in EN years there is a tendency toward TCs that are both more intense and longer-lived than in LN years. Furthermore, EN years contained more category 3-5 storms and fewer storms that do not intensify past the tropical storm phase. Recently, Camargo et al. (2007a,b) further confirmed that intense typhoons (category 3-5 on the Saffir-Simpson scale) have a higher frequency of occurrence during EN years, and mean genesis locations are much farther southeastward where the SST is above-normal.

3. Antarctic Oscillation

The Antarctic Oscillation (AAO) is a low-frequency mode of atmospheric variability of the Southern Hemisphere (SH), and represents the dominant pattern of non-seasonal tropospheric circulation variations south of 20°S. It is characterized by pressure

anomalies of one sign centered in the Antarctic and anomalies of the opposite sign centered about 40-50°S, and thus involves a large-scale alternation of atmospheric mass between the mid-latitudes and high latitudes (Gong and Wang 1999).

Thompson and Wallace (2000) found that both the AAO and its NH counterpart, the Arctic Oscillation (AO), exist year-round in the troposphere. The AAO and AO amplify with height upward into the stratosphere during certain times of the year or "active seasons." Thompson and Wallace also note that these annular modes are characterized by fluctuations in the strength of the trade winds throughout the subtropics of their respective hemispheres. While Thompson and Lorenz (2004) establish that annular modes have the largest amplitudes at extratropical latitudes (Figure 13), but they have a substantial signature in tropical latitudes as well. Thompson and Lorenz suggest that the annular modes should not be viewed as patterns of variability restricted to their respective hemispheres, but as structures that extend deep into the tropics and subtropics of the opposing hemisphere. In the tropical troposphere, the high index polarity of the annular modes is associated with westerly anomalies centered about the equator at approximately 200 hPa flanked by cool anomalies that peak in the subtropical troposphere of both hemispheres. The tropical signature of the annular modes is observed in association with both annular modes during their respective winter seasons, but has substantially larger amplitude in association with the North American Mode (NAM).
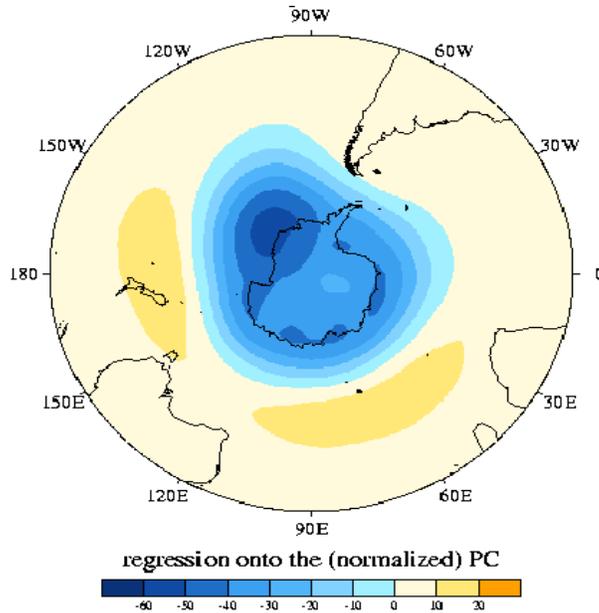
Figure 13.   EOF 1 of SH extratropical 850 hPa Z (meters), after the 850 hPa geopotential height anomalies has been regressed onto the (normalized) AAO time series. Typical fluctuations in the AAO are associated with anomalies in excess of 30 m over the pole and height anomalies of opposite sign and 5-10 m in magnitude at the latitude of New Zealand. (From: http://jisao.washington.edu/data/aao/)

Fogt and Bromwich (2006) showed that the ENSO-Antarctic teleconnection is strongest during SH (NH) spring (fall) and summer (winter). While the SH summer correlation remained unchanged over the last two decades, the spring correlation was stronger during the 1990s and weaker during the 1980s. Since the 1970s (Figure 14), the AAO index has changed toward a high polarity coincident with more frequent and stronger EN events during this time period. In contrast to the ENSO teleconnection, the AAO trend towards high polarity is strongest during the SH summer and autumn (Thompson and Solomon 2002).
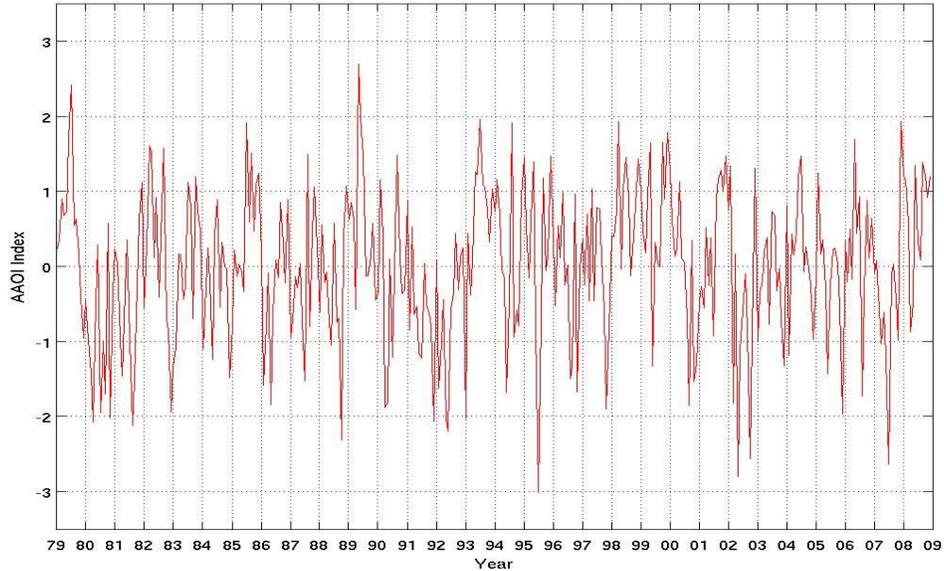
Figure 14.   AAO index from 1979 to October-2008. Above- (below-) normal events are
defined by being higher (lower) that one standard deviation ($\sigma_{AAO} = 1.073$).

Xue et al. (2004) found that the AAO dominates interannual variability of the Mascarene High (MH), which in turn has direct impacts on the strength of the Somali jet and Indian monsoon westerlies. When the circumpolar low in the high southern latitudes deepens, the intensity of the MH will be increased. On the other hand, the Australian High (AH) is impacted by ENSO as well as AAO, and the intensity of the AH will be increased when EN occurs. This pulsing of the amplitude of the AH controls the occurrence of cross-equatorial flow from the SH to the monsoon region of the WNP.

Carvalho et al. (2005) explained how composites of low frequency SST variation, 200-hPa zonal wind, and OLR indicate that negative (positive) phases of the AAO are dominant when patterns of SST, convection, and circulation anomalies resemble EN (LN) phases of ENSO. One of the primary tropical forcings of teleconnections responsible for variations in the AAO seems to be the low-frequency variability in SST modulating tropical convective patterns. Composites of SST revealed that negative (positive) AAO phases were dominant when warm (cold) SST anomalies were observed over the central–eastern Pacific. Carvalho et al. also briefly investigated the AAO's link with the MJO and concluded that negative phases of the AAO are related to the eastward propagation of intraseasonal anomalies that are able to enhance convection over the

19

central Pacific and SPCZ. Conversely, persistent positive phases of the AAO are favored in opposite conditions, i.e., when convection is suppressed near the dateline and over the SPCZ.

4. Indian Ocean Dipole

The Indian Ocean Dipole (IOD), which is also called the Indian Ocean Zonal Mode (IOZM) and the Indian Dipole Mode (IDM), is a major coupled perturbation in the tropical Indian Ocean that involves a basin-scale ocean-atmosphere interaction. Saji et al. (1999) defined this zonally out-of-phase SST anomaly pattern and its associated equatorial zonal wind anomaly. They explained in detail the process of IOD formation. First, cool SST anomalies appear in the vicinity of the Lombok Strait by May/June and are accompanied by moderate southeasterly wind anomalies in the southeastern tropical IO. A few months later, the cold anomalies intensify and migrate toward the Equator along the Indonesia coastline, while the western tropical IO begins to warm up. Zonal wind anomalies along the Equator and along-shore wind anomalies off Sumatra intensify together with the SST dipole. A dramatically rapid increase occurs in October, and then is followed by a rapid demise of the SST gradients and wind anomalies. The intensity of the SST dipole mode and the strength of the zonal wind anomaly over the Equator are strongly dependent on each other and there is a tight coupling between them. Although the IOD occurs in all seasons, it is most pronounced in the boreal summer and fall (peaking during boreal fall as mentioned above), and is closely linked to the seasonal cycle of Asian-Australian monsoon (Murphree 2008).

The positive (negative) phase of the IOD is characterized by anomalously high (low) SST, low (high) OLR, and greater (lesser) precipitation in the western tropical IO as compared to the southeastern IO near Sumatra (Figure 15).
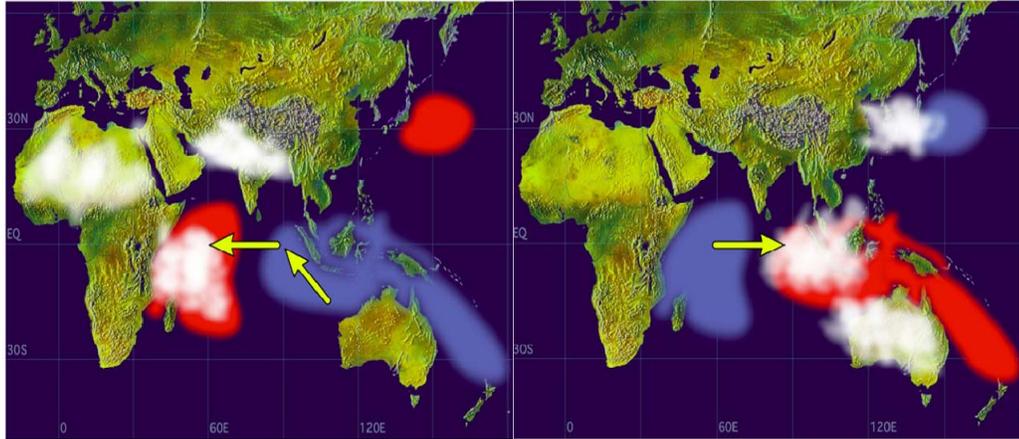
Figure 15.   Schematic of a positive IOD event (left panel) and negative IOD event (right panel). SST anomalies are shaded (red for warm anomalies and blue for cold). White patches indicate increased convective activities and arrows indicate anomalous wind directions during IOD events (From: http://www.jamstec.go.jp/frsgc/research/d1/iod/)

A significant positive IOD occurred in 1997-8 and again in 2006, and the IOD has stayed positive since. The IOD interacts with similar phenomena analogous to the ENSO, and a positive IOD phase is often associated with EN. However, the positive IOD in 2007 existed with LN, which is a very rare combination. In addition, the occurrences of consecutive positive IOD events are extremely rare. However, Saji et al. (1999) noted that the dipole mode is independent of the ENSO, and noted that the correlation between the Dipole Mode Index (DMI) and Niño3 SST anomaly time series is weak (<0.35) (Figure 16).
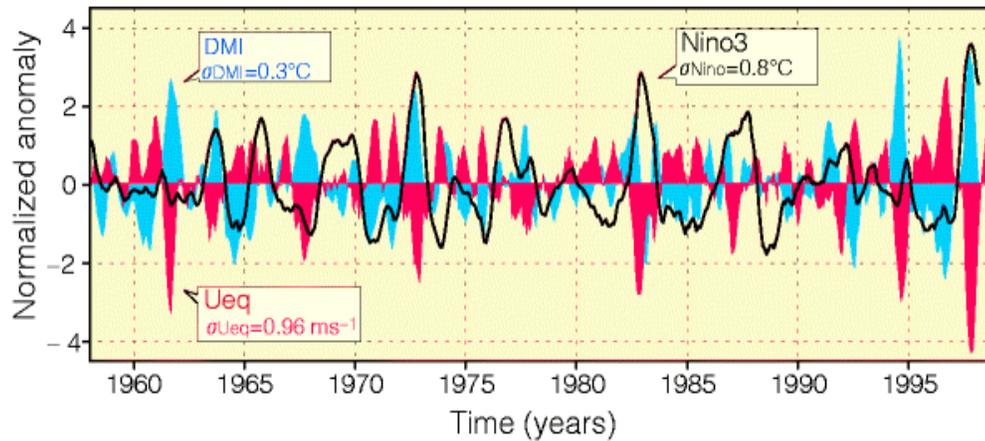
Figure 16. Dipole mode and EN events since 1958. The dipole mode index (DMI, blue) (plotted in blue) exhibits a pattern of evolution distinctly different from that of the El Niño, which is represented by the Nino3 SST anomalies (black line). On the other hand, equatorial zonal wind anomalies U_{eq} (plotted in red) coevolves with the DMI. All three time series have been normalized by their respective standard deviations. (From: http://www.ocean.washington.edu/people/faculty/susanh/423/Saji_paper/Dyna Page_002.html)

Shinoda and Han (2005) correlated the activity of subseasonal winds in the equatorial IO and the SST dipole during the boreal fall season. The wind variability on the submonthly (6-30 days) time scale was primarily responsible for the strong correlation. SST anomalies in the eastern IO could be generated by modest ENSO events through an atmospheric bridge mechanism, and the large SST anomalies could be developed through positive feedback between subseasonal and interannual variability.

The DMI from 1979 to October 2008 (Figure 17) identifies strong (above one standard deviation) positive IOD events occurred in 1982, 1987, 1991 (moderate), 1994, 1997 (moderate), and 2007; while strong (below one standard deviation) negative IOD events occurred in 1980 (moderate), 1992, 1996, and 1998.

22
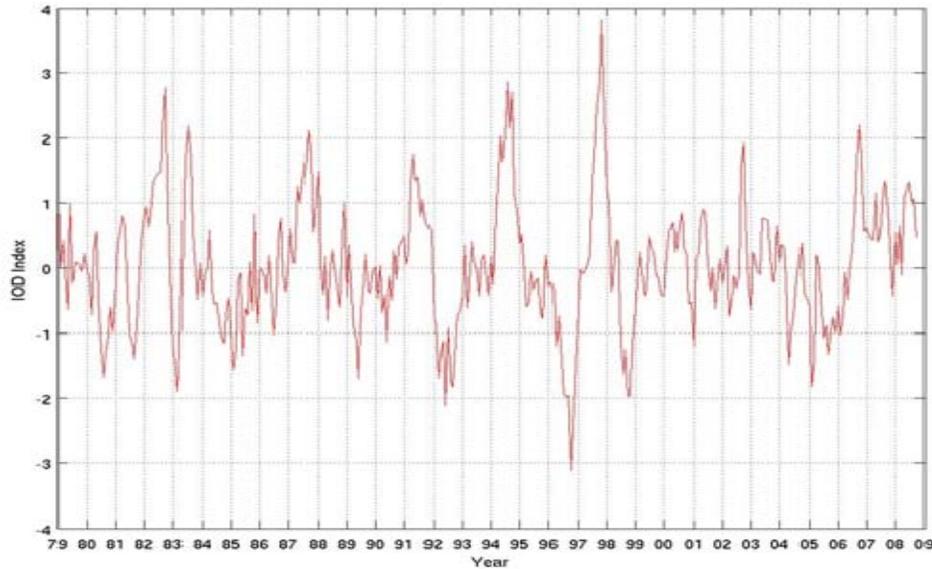
Figure 17.   Dipole Mode Index (DMI) as in Figure 16, except from 1979 to October 2008. Above- (below-) normal events are defined by been higher (lower) that one standard deviation ($\sigma_{IOD} = 1.073$).

Also of importance to naval operations is the fact that during a positive IOD the trade winds are extended well into the western IO, with an easterly component along the equator that prevents the equatorial current intrusion that allows the cooling process to dominate off the coast of Indonesia. This cooling, which is manifest by a lowering of the sea level, is further enhanced by entrainment processes associated with the coastal winds that are effective due to a shallower thermocline. On the west side of the IO, increased convergence and convection, and thus reduced wind speed and reduced evaporation, aid in increasing the SST. Entrainment is inhibited as increased rainfall increases the stability of surface waters through reduced salinity. As the thermocline in the western IO deepens due to reduced eastward transport, a positive feedback mechanism is established (Saji et al. 1999).

5.   Monsoon Trough

The monsoon trough (MT) is defined as an area between westerly monsoon winds on the equatorward side and easterly trade winds on the poleward side. The MT is an

area in which monsoon depressions and TCs form due to localized increases in the cyclonic background vorticity. This increase in vorticity is normally a product of increased wind convergence within the MT.

Low-level, vorticity-rich environments, and a 'pre-existing' near-surface disturbance lead to a better than average chance of TC formation due to their inherent rotation. Gray (1979) found that TC genesis is often grouped in clusters with 2-3 weeks of activity followed by 2-3 weeks of inactivity, which may be related to the 15-25 day cycle in convective activity in the MT (Delk 2004). Whenever the MT on the eastern side of the summertime Asian monsoon is in its normal orientation east-southeast to west-northwest, TCs along its periphery will move with a westward motion. With a reverse-oriented MT (southwest to northeast), tropical cyclones will move more poleward (Lander 1995). Wang (2006) also noted that when the MT lies near 20°N in the Pacific, the frequency of TCs is 2 to 3 times greater than when it lies closer to 10°N.

As mentioned earlier, Saji et al. (1999) stated that the changes in the state of the climate system associated with the seasonal monsoonal reversals are responsible for the demise of the dipole mode event. They noted that the dipole mode shares certain common features, such as the biennial tendency, with the monsoonal variability. Also, easterly anomalies along the Equator as well as reduced convection in the ocean tropical convergence zone (OTCZ) are well-known features of strong monsoons.

6.   Accumulated Cyclone Energy

Accumulated Cyclone Energy (ACE) is calculated by summing the squares of the estimated maximum sustained velocity (kt) of every active tropical storm (wind speed 35 kt or higher) at six-hour intervals (Bell et al. 1999). The unit of ACE is $10^4 \, kt^2$. The seasonal ACE thus takes into account the number, strength, and duration of all the TCs in the season. Although this index is biased toward the more intense TCs, it has been suggested that a slightly weaker TC lasting for a long time, or many more such weak TCs, would also contribute as much as a short-lived intense TC (Chan 2008).

The ACE index (Figure 18) is favored in many studies due to its usefulness for computing correlations and regressions with other climate variables of interest. Summation of storm intensity over the lifetime of each storm as well as over all storms is, arguably, appropriate for indexing the effect of TCs on climate (Camargo and Sobel 2005).
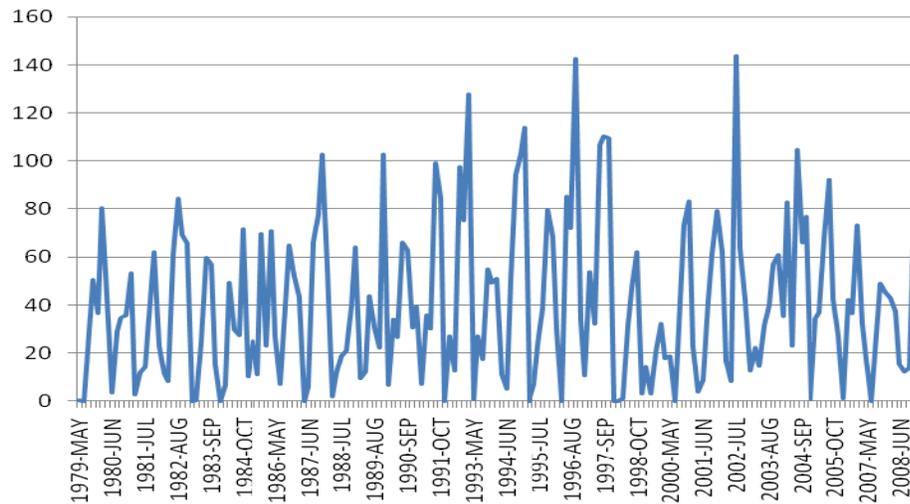
Figure 18.   Climatology of monthly ACE index for May-October 1979-2008.

A breakdown of ACE index values for each month (May-October) is depicted below (note that the ordinate changes in each diagram). The high value of ACE in May 2008 (Figure 19) is comparable to the largest values that have occurred since 1979. Although the ACE values for June and July 2008 (Figures 20 and 21) were below average, there were several previous years with similar values. In August 2008 (Figure 22), the ACE value was the lowest value to occur in the interval 1979-2008. This was also the case for October 2008 (Figure 23) while September 2008 was near average (Figure 24).
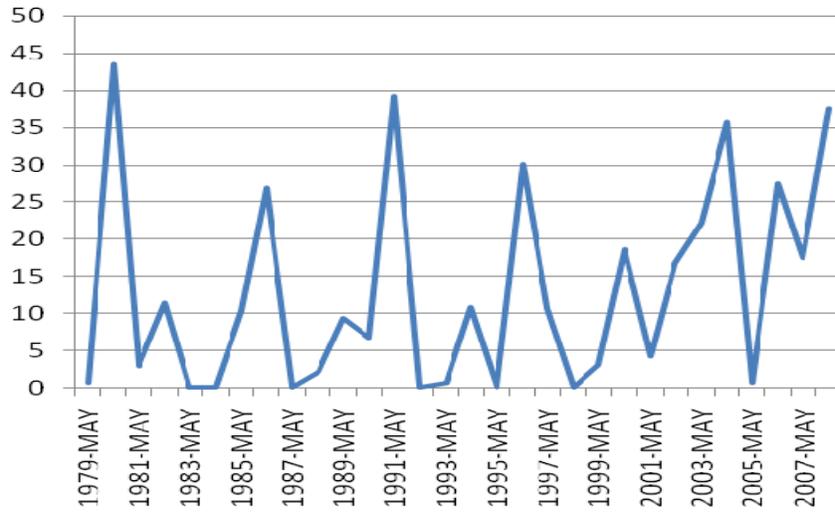
Figure 19.   May monthly ACE index from 1979-2008.
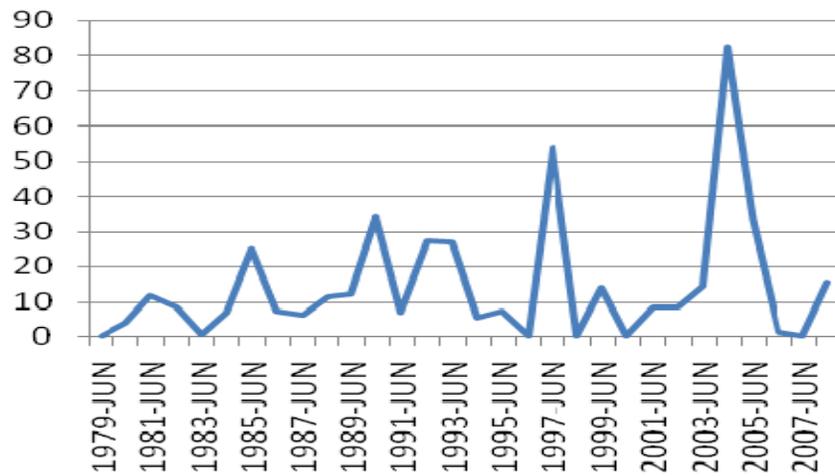
Figure 20.   June monthly ACE index for 1979-2008.
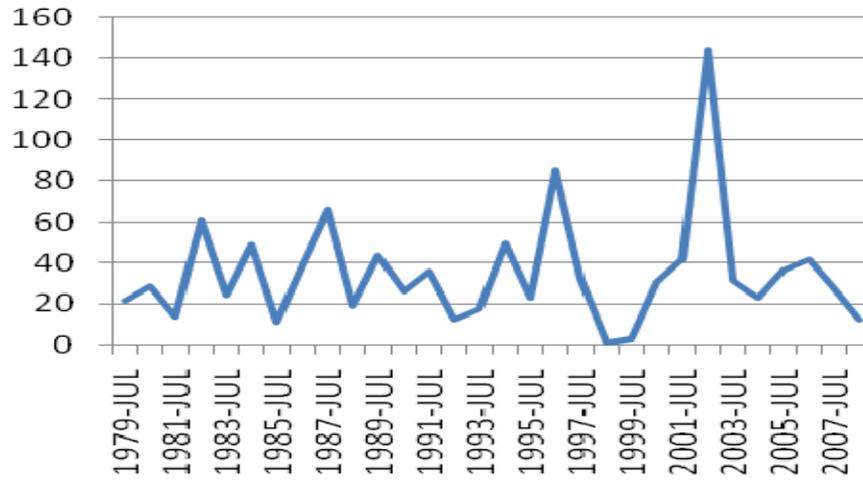
Figure 21.   July monthly ACE index from 1979-2008.
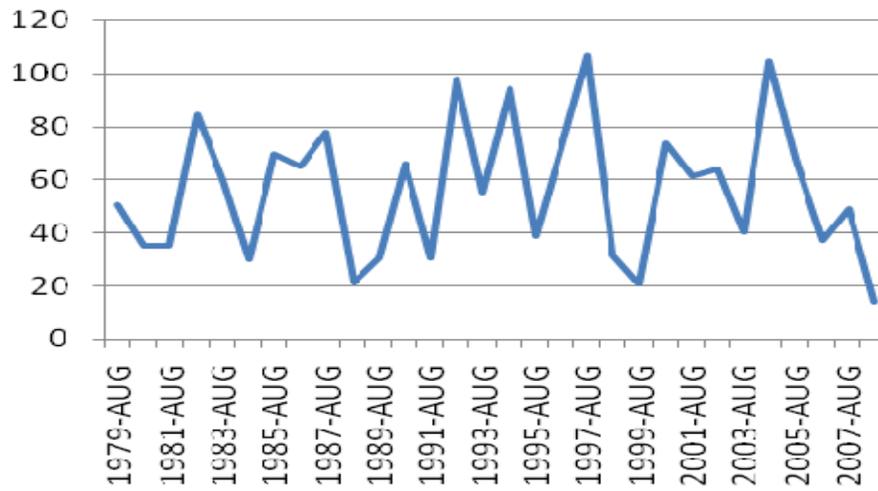
Figure 22.   August monthly ACE index from 1979-2008.

27
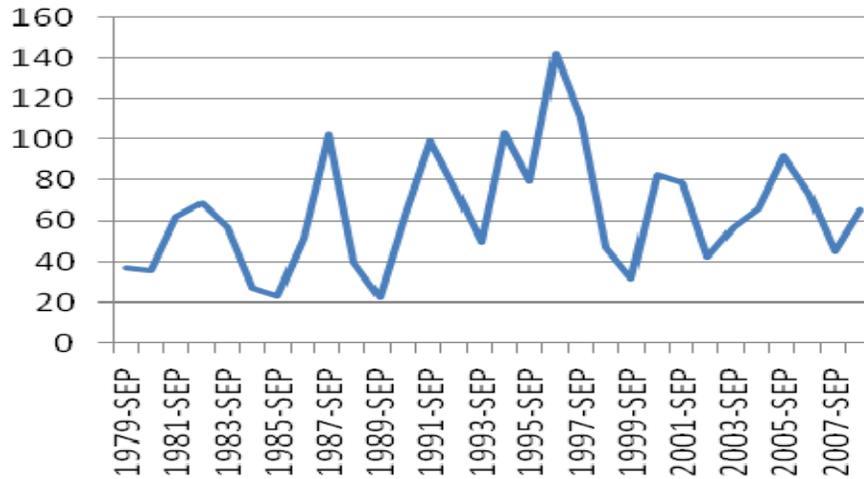
Figure 23.   September monthly ACE index from 1979-2008.
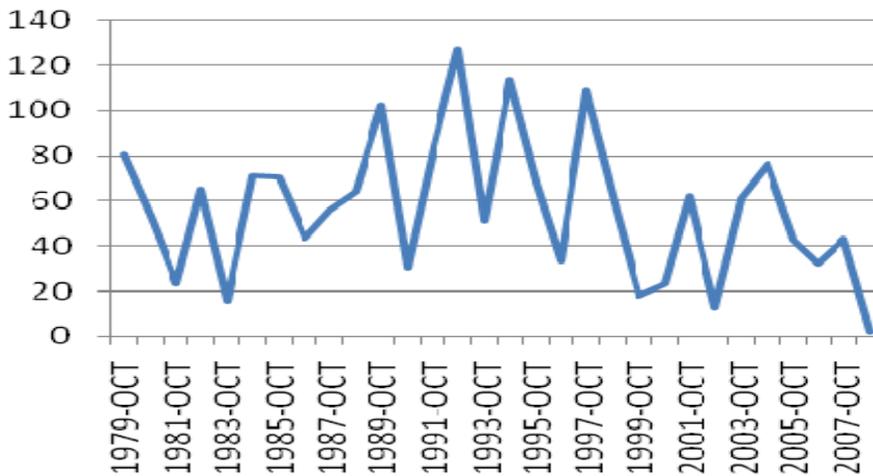
Figure 24.   October monthly ACE index from 1979-2008.

7.   Synopsis

The above summary highlights some of the predominant large-scale circulations affecting the WNP weather patterns and TC activity. They vary in space and time as mentioned earlier, and some are more dominant than others (i.e., ENSO being the strongest and leading signal in the tropics).   However, it is possible that certain combinations of these signals can enhance or decrease TC activity during certain seasons.

The working hypothesis in this study is that the number of named TCs during the WNP 2008 season was negatively influenced by an 'obstructive' combination of large-scale oscillations that were related to some degree and may have enforced (or repelled) their effects on TC activity. It has been well documented that EN (specially a strong or moderate event) supports a more active season by establishing a vast area of warm SSTs, high ocean heat content (OHC), westerly anomalies, higher moisture, and greater convection closer to the Central Pacific (CP)/dateline. In this situation, TCs are more numerous, longer-lived, more intense, and track farther west/northwest. Opposite conditions exist during strong or moderate LN conditions: moist and warm area is farther west and closer to the Asian continent and anomalies are predominately easterly. Therefore, TCs are shorter-lived, less intense, and straight-runners. The PDO signal may reinforce the already existing EN/LN event with positive (negative) PDO reinforcing EN (LN) events. A positive (negative) IOD is hypothesized to reinforce EN (LN) conditions or may be an extension of EN/LN in the IO. The AAO impacts the position and strength of the Mascarene High (MH) and consequently the MT by hindering cross-equatorial winds and westerly anomalies in the equatorward side of the MT. A negative AAO reinforces EN events, while a positive AAO opposes it. The IOD appears to be a more regional IO effect that has little direct influence on WNP TC activity.

Based on the characteristics associated with the large-scale, slow-varying circulations identified above, the following questions are investigated in this thesis:

    i.   What are the states of the large-scale circulations during the 2008 typhoon season?

    ii.   How significant was the combination of LN-like anomalies and a negative PDO even though the traditional ENSO indices did not indicate LN condition?

    iii.   What are the favorable and the unfavorable combinations for an active/inactive season?

The period of 1979-2008 is investigated to identify combinations of large-scale circulations that have significant impacts on TC activity. The conditions during 2008 are then placed into the historical perspective.

II. METHODOLOGY

A. DATA

This study is based on official TC warnings/advisories obtained from the Annual Tropical Cyclone Reports on the JTWC website (https://metocph.nmci.navy.mil/ jtwc/atcr/atcr_archive.html) for the years 1979-2008. The last 30 years were chosen as they reflect the most recent trends and have less uncertainty than previous years. Thirty years of data are also typically used for developing a climatology and for consistency in most weather parameters. The 'season' defined in this paper encompasses the months from May through October. Although this period is longer than the T-PARC/TCS-08 period, it was chosen as the large-scale anomalies were set as early as May 2008 and persisted through October 2008. Lastly, JTWC uses 1-minute winds, which is the standard in U.S. naval operations, while the Japan Meteorological Agency (JMA) uses 10-minute average winds.

Throughout the years, significant differences have existed between the warnings by JTWC and the Regional Specialized Meteorological Center (RSMC) in Tokyo. In 2008, the RSMC did not name four TCs that JTWC considered to have reached TS intensity (01W, 16W, and 22W) and TD intensity (14W). Whereas Halong was considered a typhoon by JTWC but not by RMSC, Phanfone was considered a TS by RSMC but JTWC issued no warning for that system (Camargo 2009). Because JTWC is the main TC forecast facility for all U.S. military assets, this thesis focused on their data.

Using the information above, the statistical values of certain seasons were analyzed to define strong/moderate (above or below one standard deviation) characteristics and combinations of ENSO, PDO, IOD, AAO, and MT. In this thesis, strong is defined as having five to six of the May-Oct months in the same category. Moderate was defined as having four months per season, and 'weak' as having two to three months. Neutral was defined as having zero to one month in the above-mentioned categories.

31

Combinations of large-scale oscillations and high ACE/STY values were analyzed. Initially, the factor used for pivot table combinations was the TC count for the season. However, ACE proved to be a more reliable unit for the analysis. The number of STY and the average were also considered for analysis and proved equally valuable as ACE for all circulations with the exception of MT. Each circulation index was analyzed and "above normal" was characterized by values above one standard deviation (σ), "below normal" was any value below one standard deviation (σ), and "normal" is anything in between. Based on standard classification, ENSO conditions were determined to be Above (warm) or Below (cold) if they were above the threshold of +/- 0.5^{o}C for at least five consecutive months.

A t-test was used to test the null hypothesis of various combinations: $ACE_{ENSO+} \leq ACE_{ENSO-}$, $ACE_{PDO+} \leq ACE_{PDO-}$, $ACE_{IOD+} \leq ACE_{IOD-}$, $ACE_{AAO-} \leq ACE_{AAO+}$. The alternative hypothesis would have the opposite sign (e.g., $ACE_{ENSO+} > ACE_{ENSO-}$). The results are statistically significant if the one-tailed probability [$P(T<=t)$] are less than the alpha (0.05 in this case) used. T-test was also performed on STY counts and it will be shown later that in some cases made the results even more statistically significant. A second statistical analysis compares combinations of circulations (e.g., $ACE_{ENSO+,PDO+} \leq ACE_{ENSO+, PDO-}$).

B.   MONTHLY INDICES

The ENSO monthly index was obtained from the Climatic Prediction Center (CPC) website: http://www.cpc.noaa.gov/products/analysis_monitoring/ensostuff/ ensoyears.ERSST.v3.shtml. Warm and cold episodes based on a threshold of +/- 0.5^{o}C for the Oceanic Niño Index (ONI) [3 month running mean of ERSST.v3 SST anomalies in the Niño 3.4 region (5°N-5°S, 120°-170°W)] based on the 1971-2000 base period. For historical purposes, cold and warm episodes are defined when the threshold is met for a minimum of 5 consecutive over-lapping seasons. Beginning in December 2008, the ONI is calculated using Version 3b of the extended reconstructed sea surface temperature (ERSST) dataset. This new monthly analysis replaces ERSST Version 3, which was used for this thesis and will no longer be updated (Internet).

The PDO index was obtained from the Joint Institute for the Study of the Atmosphere and Ocean (JISAO) website: http://jisao.washington.edu/pdo/PDO.latest. The values for the PDO index are derived as the leading primary component (PC) of monthly SST anomalies in the North Pacific Ocean (NPO) poleward of 20N.

The IOD index or DMI was obtained from the Japan Agency for Marine-Earth Science and Technology (JAMSTEC) website: http://www.jamstec.go.jp/frsgc/ research/d1/iod/, and is calculated as the difference of the western tropical Indian Ocean (WTIO), defined as a box of longitudes 50-70°E and latitudes 10°S-10°N, and the southeastern tropical Indian Ocean (SETIO), defined as a box of longitudes 90-110°E and latitudes 10°S-0°N indices. The AAO index was acquired from the CPC website: http://www.cpc.noaa.gov/products/precip/CWlink/daily_ao_index/aao/aao_index.html. The daily AAO index is constructed by projecting the daily (00 UTC) 700 mb height anomalies poleward of 20°S onto the loading pattern of the AAO.

Lastly, the WNP MT index for June, July, August, and September (JJAS), was obtained from the International Pacific Research Center (IPRC) website (http://iprc.soest.hawaii.edu/~ykaji/monsoon/). The MT index is defined as the difference between the 850 hPa U-wind at a box bounded by 100E-130E and 5N-15N minus the 850 hPa U-wind in a box bounded by 110E-140E and 20N-30N (Figure 25).
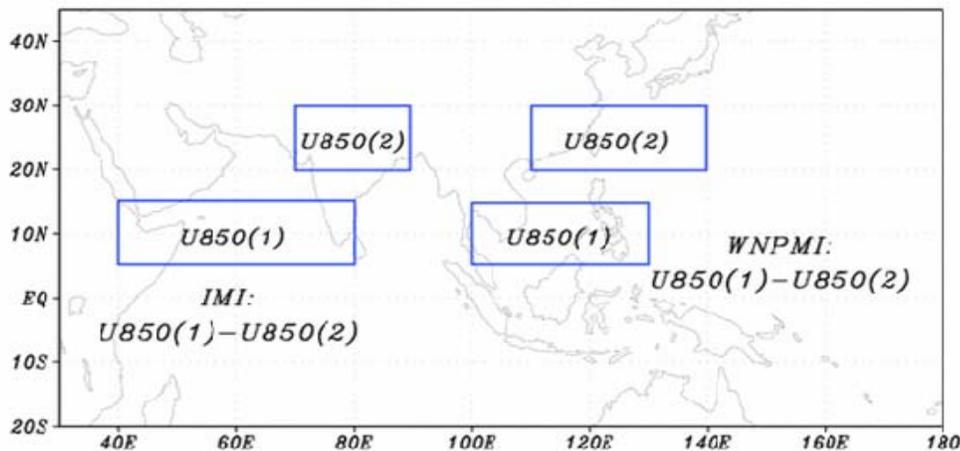
Figure 25.   Asian summer monsoons indices and definition of the WNP Monsoon Index (WNPMI) (From: http://iprc.soest.hawaii.edu/~ykaji/monsoon/definition.html).

C.   COMPOSITES

To investigate circulation characteristics related to TC activity, composites of winds (U and V components) and OLR anomalies were examined. The composites were constructed from monthly-mean reanalysis data from the National Centers for Environmental Prediction / National Center for Atmospheric Research (NCEP/NCAR). Conditional composites of seasons with similar large-scale circulations phases (e.g., positive ENSO (1-D), positive ENSO, and positive PDO (2-D), etc.) vs. opposing phases (e.g., negative ENSO (1-D), negative ENSO, and negative PDO (2-D), etc.) were plotted to highlight significant differences in ACE and STY values during opposing phases. Positive phase plots were then subtracted from negative phase plots (or vice versa for AAO) to identify differences between groups. The difference charts were subjected to local significance tests in that the difference in winds and OLR anomalies at each grid point are evaluated with a t-test to determine if it is significantly different from zero.

III.   ANALYSIS

Camargo (2009) explains that the number of TSs and TYs in the WNP basin during the 2008 season was only slightly below the median, i.e., almost the normal number of TCs formed, but very few of them reached TY intensity. Therefore, the low activity this year was due in part to the lack of intensification and not as much to the lack of genesis in the region. The ACE values early in the year were in the top 10th percentile of the climatological distribution, while the ACE values for the peak season (July-October) were in the bottom 5th percentile. Indeed, 2008 had the third lowest seasonal ACE value since 1979. The objective of this section is to attempt to explain this deficient TC activity in terms of the various large-scale circulations.

As previously described in Chapter I.C.2., low values of ACE usually occur in LN years when the WNP TCs tend to be short-lived and less intense. Since the mean genesis location and mean tracks are shifted northwest of the climatological mean positions during LN events, this leads to shorter-lived and weaker than normal TCs (Wang and Chan 2002; Camargo and Sobel 2005; Camargo et al. 2007b). According to many ENSO indices, 2008 was characterized to be an ENSO neutral year that followed a moderate LN event that ended in May. Other indices, such as Niño4 SST index, suggested that the cold event never ended in 2008 despite warming in the eastern Pacific. Additionally, the Southern Oscillation Index (SOI) was briefly neutral during the summer months, but has been positive since September.

As mentioned in Chapter II, the PDO signal was strongly negative throughout the 2008 typhoon season, the IOD and AAO were both weakly positive (a positive AAO is related to an inactive TC season), and the eastern portion of the MT was confined to a small region west of the Philippines (Camargo 2009). Camargo explains that the genesis potential index (GPI) during 2008 was above normal in the WNP and below normal near the date line and in the SCS, which is consistent with the presence of LN. Other seasons similar to 2008 will be studied below by analyzing seasonal composites, and examining Asian-Australian Monsoon data from the CPC website.

A.   STATISTICAL ANALYSIS OF CIRCULATION INDICES

1.   Individual Indices

A summary of seasonal TC activity, ACE values, large-scale circulation categories, and MT index (as defined in Chapter II) from 1979 to 2008 is given in Table 2. The Above and Below categories of the large-scale circulation are more than or less than one standard deviation from the mean values over the period 1979 to 2008. Table 3 contains the average ACE values for the three standard categories of each large-scale circulation and the differences between the two extreme states.

Table 2.   Yearly (May-October) TC activity from 1979-2008 divided into supertyphoons (STY), typhoons (TY), tropical storms (TS), and tropical depressions (TD) in relation to the seasonal (May to October) large-scale circulations categories. Seasonal and yearly ACE values and WNP MT index (June to September) are also included. Red shading indicates above one standard deviation, while blue shading indicates below one standard deviation.

YEAR	ENSO	PDO	IOD	AAO	MT	STY	TY	TS	TD	STORM TOTAL	MAY-OCT ACE	YEAR ACE	MT (JJAS) INDEX
1979	Neutral	Neutral	Neutral	Above	Neutral	3	6	7	4	20	189.67	278.36	-0.213
1980	Neutral	Above	Below	Below	Neutral	2	12	7	3	24	200.07	237.95	-0.189
1981	Neutral	Above	Below	Below	Neutral	1	10	9	1	21	148.78	227.78	0.457
1982	Above	Neutral	Above	Neutral	Neutral	2	13	6	2	23	299.49	356.35	1.068
1983	Above	Above	Above	Above	Below	4	6	7	2	19	156.82	219.70	-1.971
1984	Neutral	Neutral	Neutral	Neutral	Neutral	1	11	11	3	26	184.42	274.74	0.248
1985	Below	Neutral	Neutral	Above	Above	1	15	5	1	22	209.14	231.09	1.405
1986	Above	Above	Neutral	Neutral	Above	2	12	6	0	20	233.52	334.90	1.307
1987	Above	Above	Above	Neutral	Neutral	5	10	4	1	20	308.09	357.20	-0.406
1988	Below	Neutral	Neutral	Neutral	Below	1	10	12	1	24	156.94	214.78	-2.207
1989	Neutral	Neutral	Neutral	Above	Neutral	3	13	10	3	29	220.53	306.13	-0.091
1990	Neutral	Neutral	Neutral	Below	Above	1	15	8	1	25	226.39	381.57	1.474
1991	Above	Neutral	Above	Below	Neutral	3	13	5	2	23	295.94	414.26	0.524
1992	Above	Above	Below	Below	Neutral	4	14	9	0	27	340.12	473.20	-0.039
1993	Neutral	Above	Neutral	Above	Neutral	3	14	7	3	27	200.43	253.16	-0.885
1994	Above	Below	Above	Neutral	Above	6	13	14	4	37	377.61	445.93	1.347
1995	Below	Above	Neutral	Above	Below	5	10	8	5	28	217.06	261.79	-1.31
1996	Neutral	Above	Below	Below	Below	5	15	6	5	31	363.02	426.15	-1.113
1997	Above	Above	Above	Neutral	Neutral	9	11	6	2	28	422.63	589.92	0.094
1998	Below	Below	Neutral	Neutral	Below	3	5	5	7	20	141.37	156.46	-2.857
1999	Below	Below	Neutral	Above	Neutral	1	8	8	6	23	90.81	108.23	-0.14
2000	Below	Below	Neutral	Neutral	Neutral	4	10	9	8	31	228.61	244.41	-0.111
2001	Neutral	Below	Neutral	Above	Above	2	15	5	2	24	257.03	315.84	1.182
2002	Above	Neutral	Above	Below	Neutral	6	8	8	5	27	286.94	352.43	1.039
2003	Neutral	Neutral	Neutral	Neutral	Neutral	3	11	4	4	22	226.29	337.41	-0.244
2004	Above	Neutral	Neutral	Above	Neutral	4	14	5	2	25	388.60	482.09	0.848
2005	Neutral	Above	Neutral	Neutral	Neutral	3	11	4	1	19	274.65	309.95	0.437
2006	Above	Neutral	Above	Neutral	Neutral	4	6	8	3	21	213.41	270.31	0.417
2007	Below	Neutral	Above	Below	Neutral	4	6	6	2	18	182.10	220.08	-0.861
2008	Neutral	Below	Above	Above	Neutral	2	8	8	3	21	146.29	168.53	-1.098
Average:	0.144	0.407	0.122	0.003	-0.063	3.23	10.83	7.23	2.87	24.17	239.56	308.36	-0.063
Std. Dev.:	0.723	1.078	1.126	1.073	1.11	1.85	3.09	2.40	1.98	4.33	81.51	106.92	1.11

When the ACE is divided into tercile categories for each large-scale circulation, the peak ACE values correspond to Above categories of ENSO, PDO, IOD, and MT, and Below category of AAO (Table 3). Therefore, these large-scale circulation relationships with ACE values through October 2008 are consistent with previous studies (Chan et al. 1998, etc.) that used different periods. The same relationships are observed using STY counts versus ACE values (Table 4). Interestingly, the MT displays higher ACE values during Above phases, but not STY numbers, which means that the MT strength is influential in TC activity, but not on the eventual maximum intensity.

The differences among ACE values and STY numbers for various index categories in Table 3 were analyzed to determine which circulations exhibited significant influence on ACE values and STY numbers. Only the ACE and STY differences between EN (ACE = 302.11, STY average = 4.55/year) and LN (ACE=175.15, STY average = 2.71/year) were significant at a 95% level of confidence. While differences in ACE values and STY numbers between years in opposite phases of PDO, IOD, AAO, and MT exist, none of these differences were statistically significant.

The individual large-scale circulations analyses provide evidence that ENSO is the dominant influence on the ACE values in any particular season, and the PDO, MT, AAO, and IOD had progressively small influences on the ACE values (Tables 3 and 4). The differences in average ACE values between positive and negative phases of each large-scale circulation were: 126.96 for ENSO, 53.70 for MT, 53.52 for PDO, 47.78 for AAO, and 5.93 for IOD (Table 3). For average STY, the differences in values were: 1.74 for ENSO, 1.50 for IOD, 0.91 for PDO, 0.45 for AAO, and -1.2 for MT (Table 4). These results reinforce that ENSO is the dominate influence on seasonal TC activity and that MT is influential in TC activity, but not TC intensity. However, the other indices may exert some influence as in 2008 when ENSO was either neutral or weak LN, but PDO was slightly negative.

Table 3.   Average ACE values from 1979-2008 (May to October) in tercile categories for each large-scale circulation studied.

Values	ENSO Above	Neutral	Below	Grand Total	Difference Between ACE
Average of MAY-OCT	**302.11**	219.80	**175.15**	239.56	**126.96**
Count of MAY-OCT	11.00	12.00	7.00	30.00	
Values	PDO Above	Neutral	Below	Grand Total	
Average of MAY-OCT	**260.47**	236.91	**206.95**	239.56	**53.52**
Count of MAY-OCT	11.00	13.00	6.00	30.00	
Values	IOD Above	Neutral	Below	Grand Total	
Average of MAY-OCT	**268.93**	215.34	**263.00**	239.56	**5.93**
Count of MAY-OCT	10.00	16.00	4.00	30.00	
Values	AAO Below	Neutral	Above	Grand Total	
Average of MAY-OCT	**255.42**	255.59	**207.64**	239.56	**47.78**
Count of MAY-OCT	8.00	12.00	10.00	30.00	
Values	MT Above	Neutral	Below	Grand Total	
Average of MAY-OCT	**260.74**	242.39	**207.04**	239.56	**53.70**
Count of MAY-OCT	5.00	20.00	5.00	30.00	

Table 4.   As in Table 3, except for the STY counts instead of ACE values.

Values	ENSO Above	Neutral	Below	Grand Total	Difference Between STY
Average of STY	**4.45**	2.42	**2.71**	3.23	**1.74**
Count of STY2	11.00	12.00	7.00	30.00	
Values	PDO Above	Neutral	Below	Grand Total	
Average of STY	**3.91**	2.77	**3.00**	3.23	**0.91**
Count of STY2	11.00	13.00	6.00	30.00	
Values	IOD Above	Neutral	Below	Grand Total	
Average of STY	**4.50**	2.50	**3.00**	3.23	**1.50**
Count of STY2	10.00	16.00	4.00	30.00	
Values	AAO Below	Neutral	Above	Grand Total	
Average of STY	**3.25**	3.58	**2.80**	3.23	**0.45**
Count of STY2	8.00	12.00	10.00	30.00	
Values	MT Above	Neutral	Below	Grand Total	
Average of STY	**2.4**	3.35	**3.6**	3.23	**-1.2**
Count of STY2	5	20	5	30	

2.   Combinations of Circulations

Table 5 is a summary of months (May to October multiplied by 30 years = 180 months) that have different combinations of large-scale circulations. The vast majority of months are characterized as having Neutral conditions. However, a tendency exists for ENSO, PDO, IOD, and AAO to dominate in the Above category (i.e., more months in the Above status than the Below category).

Table 5. Monthly count for various large-scale circulations combinations (e.g., ENSO vs. PDO, PDO vs. AAO, etc.) that fall in Above (A), Neutral (N), and Below (B) terciles.

Count of PDO	ENSO				Count of PDO	IOD			
PDO	A	N	B	Grand Total	PDO	A	N	B	Grand Total
A	16	25	2	43	A	13	27	3	43
N	29	64	22	115	N	18	78	19	115
B	3	11	8	22	B	5	15	2	22
Grand Total	48	100	32	180	Grand Total	36	120	24	180
Count of IOD	ENSO				Count of AAO	IOD CAT			
IOD	A	N	B	Grand Total	AAO CAT	A	N	B	Grand Total
A	27	7	2	36	A	5	24	2	31
N	20	76	24	120	N	26	81	15	122
B	1	17	6	24	B	5	15	7	27
Grand Total	48	100	32	180	Grand Total	36	120	24	180
Count of AAO	ENSO CAT				Count of AAO	PDO CAT			
AAO CAT	A	N	B	Grand Total	AAO CAT	A	N	B	Grand Total
A	4	19	8	31	A	8	17	6	31
N	35	65	22	122	N	28	81	13	122
B	9	16	2	27	B	7	17	3	27
Grand Total	48	100	32	180	Grand Total	43	115	22	180
Count of ENSO	Monsoon Trough				Count of PDO	Monsoon Trough			
ENSO	A	N	B	Grand Total	PDO	A	N	B	Grand Total
A	2	8	1	11	A	1	7	3	11
N	2	9	1	12	N	2	10	1	13
B	1	3	3	7	B	2	3	1	6
Grand Total	5	20	5	30	Grand Total	5	20	5	30
Count of IOD	Monsoon Trough				Count of AAO	Monsoon Trough			
IOD	A	N	B	Grand Total	AAO	A	N	B	Grand Total
A	1	8	1	10	A	2	6	2	10
N	4	9	3	16	N	2	8	2	12
B	0	3	1	4	B	1	6	1	8
Grand Total	5	20	5	30	Grand Total	5	20	5	30

These two-dimensional combinations for each large-scale circulation were analyzed to examine their impact on TC activity. Ignoring values where the combinations occurred during only one year, it is apparent that for ENSO, PDO, and IOD the highest average ACE/STY values occurred during combinations of positive phases, while the lowest values occurred during years with a negative phase. For AAO, the higher ACE values were associated with the negative phase of the circulation index.

To examine the influence of each circulation on TC activity, a null hypothesis for ENSO, PDO, and IOD is that the ACE values during positive (Above) years are equal or less than ACE values for ENSO, PDO, and IOD in negative (Below) years (e.g., $ACE_{ENSO+} \leq ACE_{ENSO-}$). The alternate hypothesis is that ACE values for positive ENSO, PDO, and IOD years are greater than the negative years (e.g., $ACE_{ENSO+} > ACE_{ENSO-}$). For AAO, the signs associated with each hypothesis are reversed. The tests were also performed on moderate and strong events for ENSO only because of its dominance over all other signals. The result is considered to be statistically significant if the one-tailed probability is less than 0.05 (Dretzke 2001).

Table 6.	Statistically significant combinations of large-scale circulations and the corresponding years of occurrences and average ACE/STY comparisons. Blue highlight indicates statistically significant values in both ACE and STY values; while yellow highlight indicates significant values of ACE only.

Categories: (N) = number of cases per category Highlighted = Statistically Significant	Years in each Category	MAY-OCT ACE Comparisons	STY Comparisons
EN (11) vs. LN (7)*	(1982, 1983, 1986, 1987, 1991, 1992, 1994, 1997, 2002, 2004, 2006) vs. (1985, 1988, 1995, 1998, 1999, 2000, 2007)	302.11 vs. 175.15	4.45 vs. 2.71
PDO+ (11) vs. PDO- (6)		260.47 vs. 206.95	3.91 vs. 3.00
IOD+ (10) vs. IOD- (4)		268.93 vs. 263.00	4.5 vs 3.00
AAO- (10) vs. AAO+ (8)		255.42 vs. 207.64	3.25 vs. 2.80
MT+ (5) vs. MT- (5)		260.74 vs. 207.04	2.4 vs. 3.6
EN only (6) vs. LN only (4)	(1982, 1991, 1994, 2002, 2004, 2006) vs. (1985, 1988, 1995, 2007)	310.33 vs. 191.31	4.33 vs 2.75
PDO+ only (5) vs. PDO- only (2)		237.39 vs. 201.66	2.8 vs 2.0
EN/PDO+ (5) vs. LN/PDO- (3)*	(1983, 1986, 1987, 1992, 1997) vs. (1998, 1999, 2000)	292.24 vs. 153.60	4.8 vs. 2.67
EN/PDO+ (5) vs. EN only (6)		292.24 vs. 310.33	4.8 vs. 4.33
LN only (4) vs. LN/PDO- (3)		191.31 vs. 153.60	2.75 vs. 2.67
EN/PDO+ (2) vs. LN/PDO- (2) (Moderate & Strong only)	(1987, 1997) vs. (1998, 1999)	365.36 vs. 116.09	7.0 vs. 2.0
EN/AAO- (3) vs. LN/AAO+ (3)*	(1991, 1992, 2002) vs. (1985, 1995, 1999)	307.67 vs. 172.34	4.33 vs. 2.33
PDO+/AAO- (4) vs. PDO-/AAO+ (3)		263.00 vs. 164.71	3.0 vs. 1.67
EN/MT+ (2) vs. LN/MT- (3)	(1986, 1994) vs. (1988, 1995, 1998)	305.56 vs. 171.79	4.0 vs. 3.0
EN/PDO+/IOD+ (3) vs. LN/PDO-/IOD (3)		295.85 vs. 153.60	6.0 vs. 2.67
EN/PDO+/AAO- (4) vs. LN/PDO-/AAO+ (3)*	(1986, 1987, 1992, 1997) vs. (1998, 1999, 2000)	330.77 vs. 153.60	5.0 vs. 2.67
EN/PDO+/IOD+/AAO (2) vs. LN/PDO-/IOD/AAO+ (3)	(1987, 1997) vs. (1998, 1999, 2000)	365.36 vs. 153.60	7.0 vs. 2.67

The only differences in ACE and STY between years with positive and negative ENSO are significant (Table 6). The difference in ACE was largest for the four years in which strong or moderate ENSO conditions existed (Table 6). Although higher ACE/STY values were found for positive PDO and for positive IOD and negative AAO, by themselves the differences between years in positive and negative phases are not

statistically significant for the available sample sizes (Table 6). The P(T≤t) one-tail test for the three-dimensional combinations was only statistically significant when a negative AAO was involved (along with a positive ENSO and positive PDO), but not when it was removed and replaced by the IOD. That is, the AAO plays a more significant role in TC activity for the Pacific basin than the IOD, which is a more regional effect in the Indian Ocean. If only years in which the positive or negative ENSO phases occurred without phases of any other circulations are considered (EN only, LN only in Table 6), the difference between ACE values in positive and negative ENSO phases is also significant. Therefore, when each circulation is examined alone only ENSO exhibits significant impact on TC activity as measured by ACE and STY .

B. COMPOSITES

To examine roles of various circulations on TC activity, the combinations that exhibit significant impacts on TC activity in Table 6 are examined by compositing upper- and lower-level wind anomalies and OLR anomalies (OLRA). Composites of anomalous winds at 850 hPa and OLRA for years of EN (11 cases) versus LN (7 cases) were examined (Figure 26) along with their difference. The anomalies for each state and for their differences were examined at each grid point to determine if they were significantly different. Only those that were significant are plotted. During positive ENSO years (Figure 26a), the 850-hPa wind anomalies are westerly in the equatorial central Pacific. The OLRA is negative in most of the central Pacific and positive over the Maritime Continent. Furthermore, the MT is stronger and more pronounced over the Philippine Sea, cross-equatorial winds are weak from the Mascarene High (MH), but strong over the WNP in association with the stronger AH, and a larger number of STY (49 vs. 19) formed over the WNP. On the other hand, negative ENSO years tend to have easterly wind anomalies west of the dateline, positive OLR over the equatorial central Pacific and negative OLR over the Maritime Continent, a prominent anticyclone over the WNP that inhibits cyclone formation, and another anticyclone over central North Pacific (Figure 26b) dominates the region. The MT in the WNP is much weaker during LN years because of weak or non-existent cross-equatorial winds from the AH, even though the cross-equatorial winds from the MH are strong farther to the west.

42

These are recurring events during years that also have PDO, IOD, and AAO, but they appear to intensify the effects (e.g., stronger westerly anomalies during a positive ENSO and positive PDO year) as will be demonstrated later. The resulting difference between EN and LN years (Figure 26c) is weak westerlies, as well as an area of strongly negative OLR differences (representing more deep convection) over most of the equatorial central Pacific and positive OLR differences (more clear skies than normal) over the Maritime Continent and southeastern IO.

At the 200-hPa level, there are weak easterly wind anomalies in the equatorial Pacific and a weak anticyclone in the WNP during positive ENSO years (Figure 27a), while weak westerly wind anomalies prevail over the equatorial Pacific during negative ENSO years (Figure 27b). The difference composite indicates weak easterly wind anomalies and a weak anticyclone over the WNP (Figure 27c). The ENSO OLR and 850- and 200-hPa (Figures 26 and 27) were used as the control or baseline to compare with other composite charts.

During years when only positive and negative ENSO exist without significant phases of the other circulations (Figure 28), the characteristics identified above are amplified. For Neutral PDO years, the EN years (Figure 28a) have strong westerlies relative to the LN years (Figure 28b). Westerly (easterly) anomalies exist over the equatorial WNP during positive (negative) ENSO phases, which are related to a strong (weak) MT over the Philippine Sea. Only differences between positive and negative ENSO that occurred over the equatorial Pacific are statistically significant (Figure 28c). Thus, the difference composite (Figure 28c) has a broader region of significant equatorial westerlies in the WNP, which indicates a more favorable environment for TC formation during the EN years. Similar characteristics are found at the 200-hPa level (Figure 29). Wind anomalies at low (upper) levels identify anomalous convergence (divergence) over the Maritime Continent during positive (negative) ENSO phases (Figure 29a,b). Statistically significant differences in upper-level wind anomalies between positive and negative ENSO only phases only occur over the equatorial Pacific (Figure 29c).
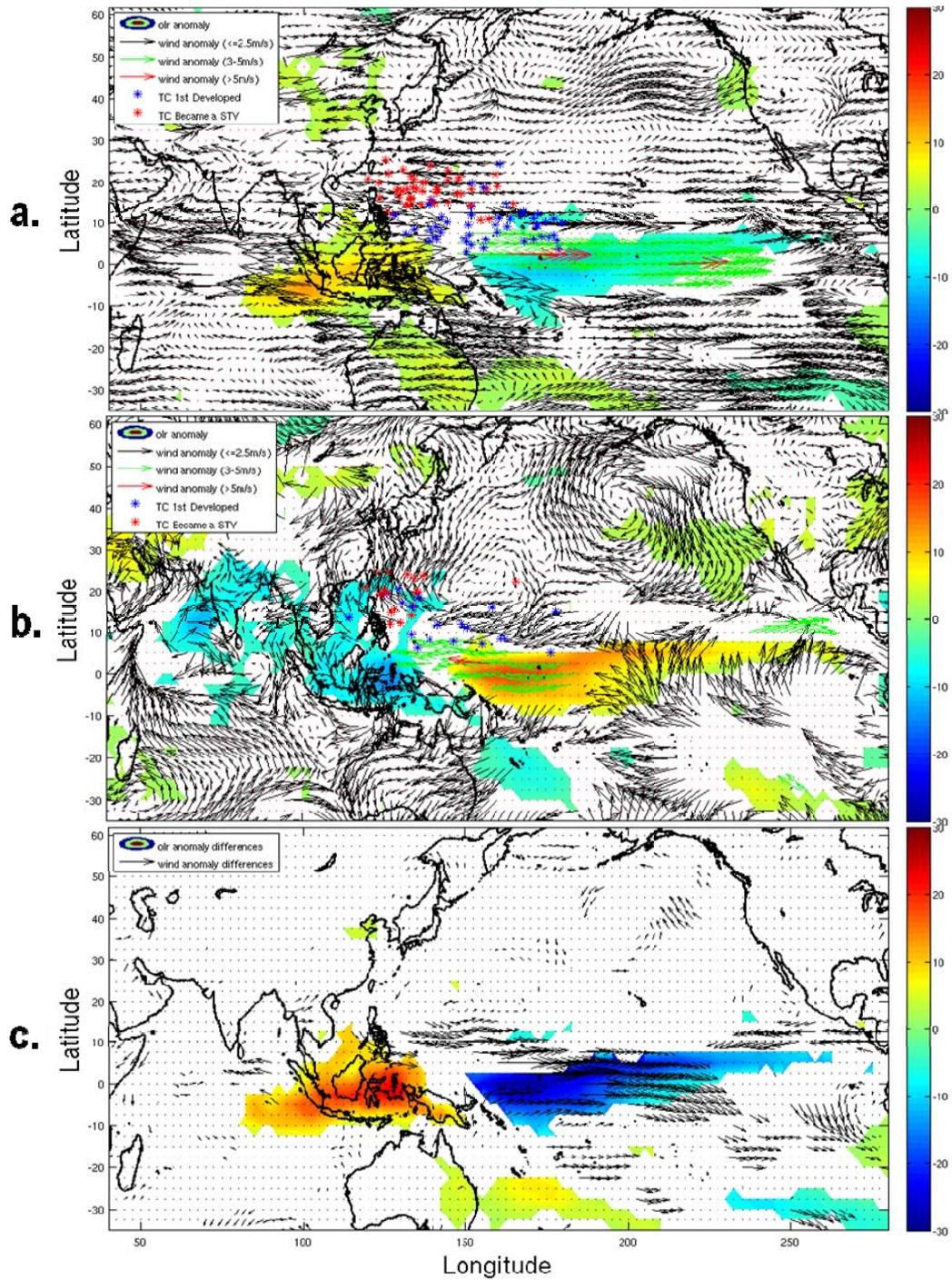
Figure 26.   Composites of OLR (shaded, W/m^2) and 850-hPa winds (vectors, m/s) during
(a) ENSO positive (11) years, (b) ENSO negative (7) years, and (c) their
difference. Blue markers identify TC formation locations of TCs that reached
STY category. The red markers identify locations where the TCs achieved
STY intensity.
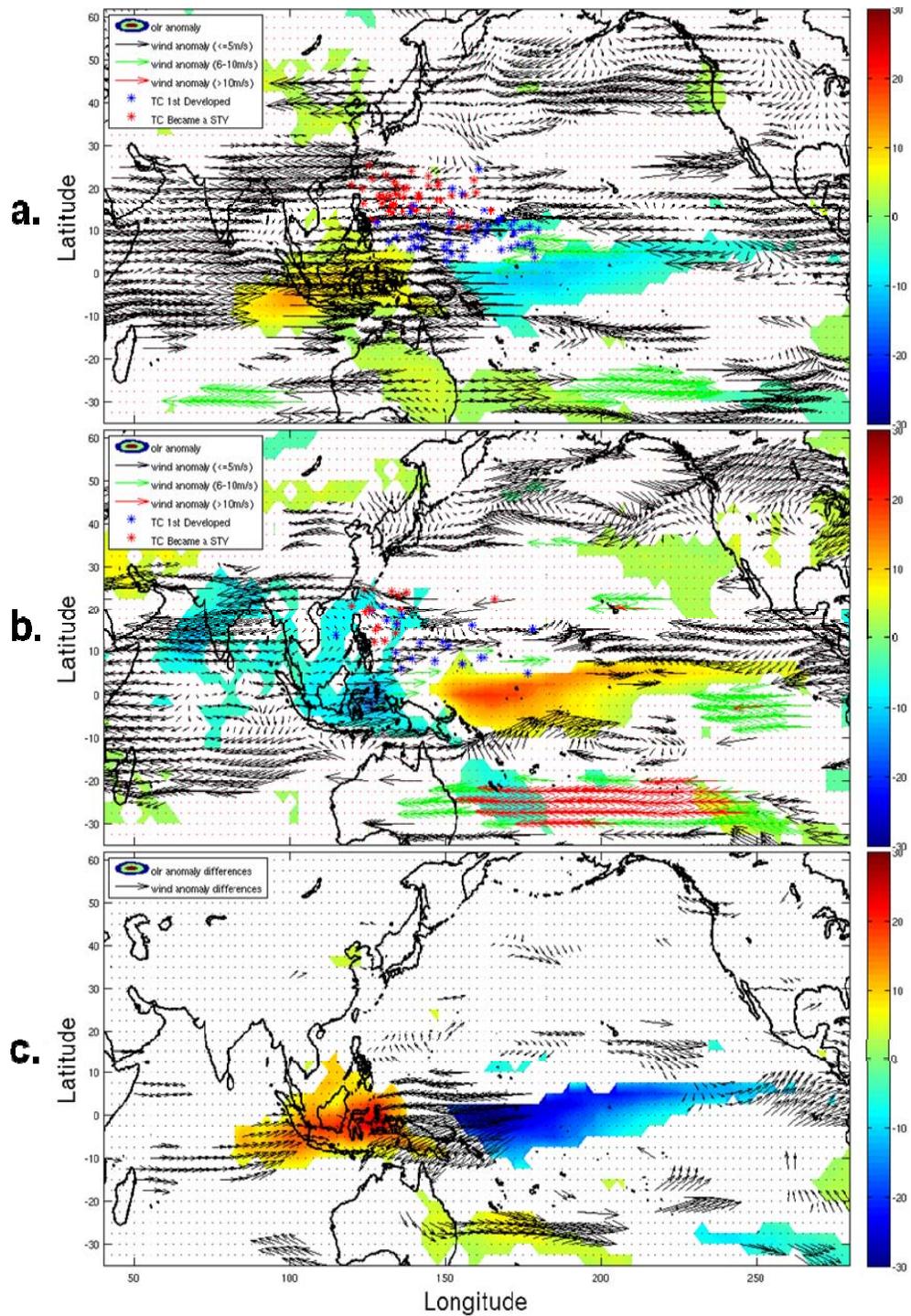
Figure 27.   As in Figure 26, except OLR (shaded, W/m^2) with 200-hPa winds (vectors, m/s). Blue markers identify TC formation locations of TCs that reached STY category. The red markers identify locations where the TCs achieved STY intensity.
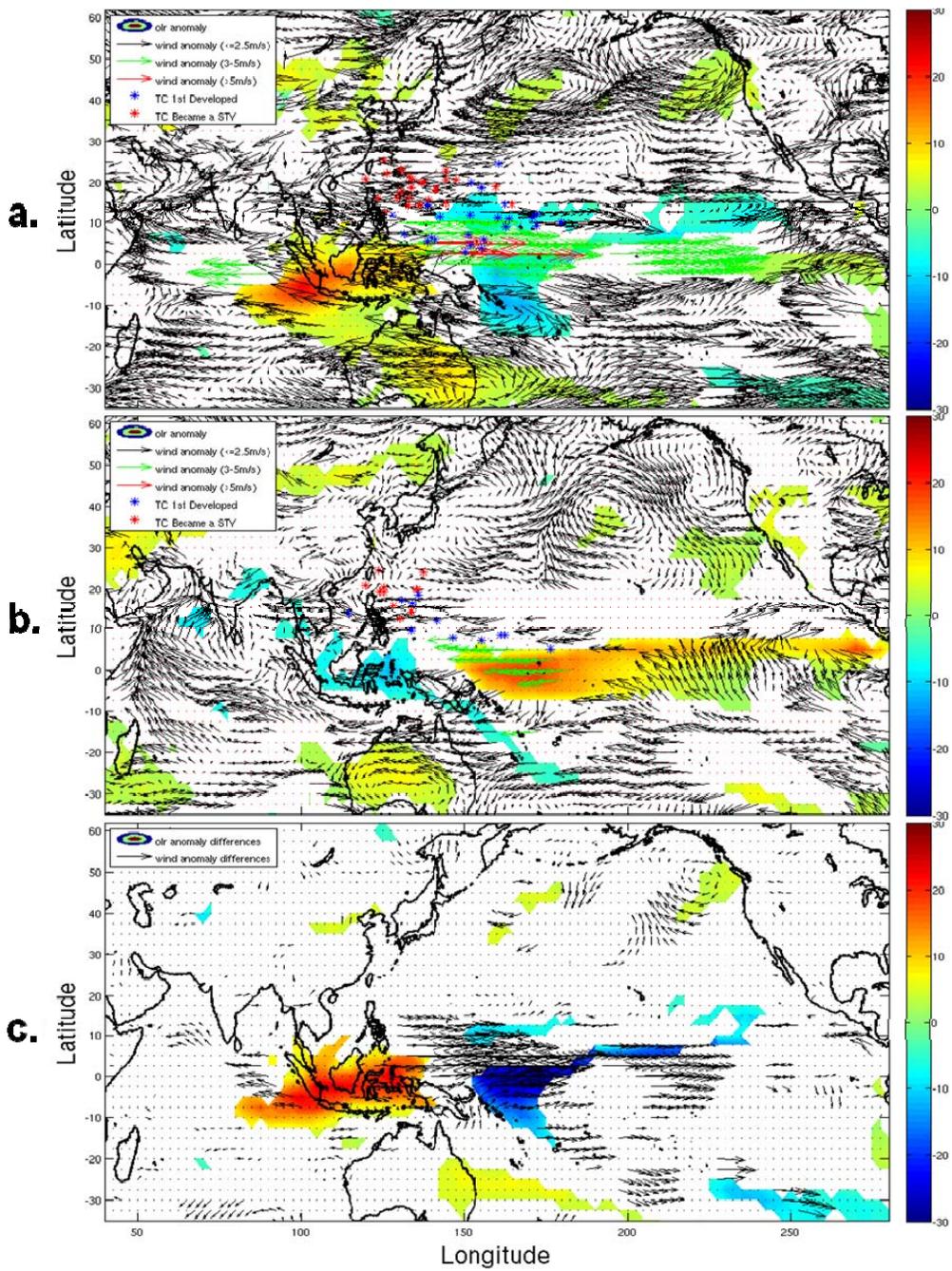
Figure 28.   As in Figure 26, except for (a) positive ENSO only (Neutral PDO) years (6), (b) negative ENSO only (Neutral PDO) years (4), and (c) their differences. Blue markers identify TC formation locations of TCs that reached STY category. The red markers identify locations where the TCs achieved STY intensity.
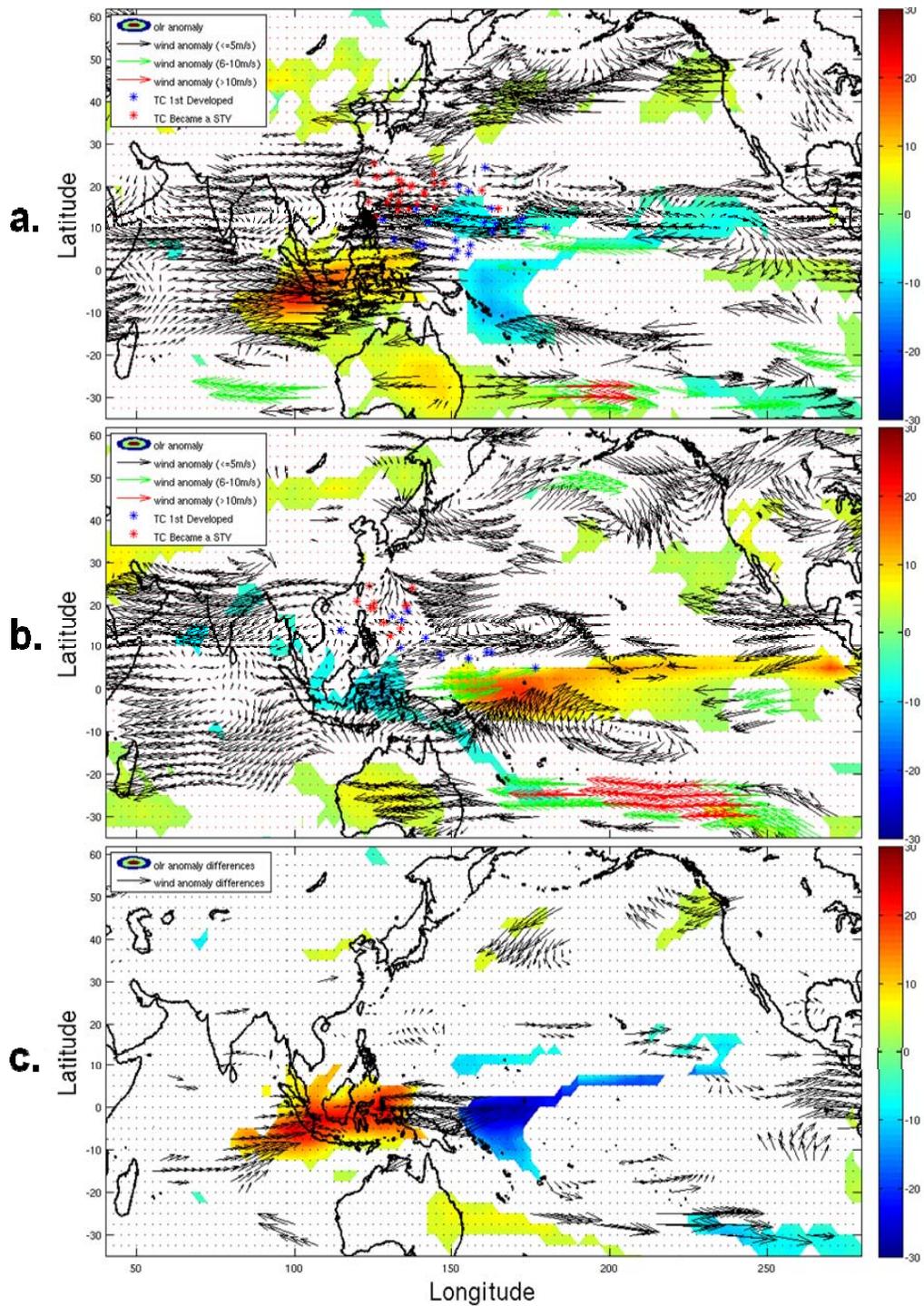
Figure 29.   As in Figure 28, except OLR (shaded, W/m^2) with 200-hPa winds (vectors, m/s). Blue markers identify TC formation locations of TCs that reached STY category. The red markers identify locations where the TCs achieved STY intensity.

Years in which the PDO is positive, or negative in conjunction with positive and negative ENSO (Figures 30 and 31), lead to positive and negative phases that have more pronounced effects on OLRA and winds. For example, the composite of positive ENSO and positive PDO has stronger westerly anomalies in the lower levels (Figure 30a) coincident with negative OLRA over the equatorial central Pacific. The cyclonic anomaly in the eastern North Pacific is much more pronounced as well as the cyclonic anomaly over the WNP. The cross-equatorial winds from the AH are also much stronger than the positive ENSO composite (Figures 26a and 28a). The opposite tendencies occur for the composite of the negative ENSO and negative PDO years (Figure 30b). Easterly anomalies occur over the equatorial Pacific with negative OLRA over the Maritime Continent. The anticyclonic anomaly over the eastern North Pacific is indicative of negative PDO conditions. The difference composite has weak westerly anomalies over the equatorial WNP that extend farther east (Figure 30c). This low-level anomaly pattern signifies an anomalous active MT over the Philippine Sea during EN/PDO+ conditions.

In the EN/PDO+ 200-hPa chart (Figure 31a), a strong anticyclonic anomaly is present over the WNP, which is complementary to the low-level MT and OLRA over this region and favors cyclone formation/intensification. By contrast, the LN/PDO- chart (Figure 31b) has a slightly more cyclonic anomaly over the WNP at the upper levels. The difference composite (Figure 31c) still has an anticyclonic anomaly over the WNP, which suggests that the upper-level anticyclone anomaly in EN years is stronger than the cyclonic anomaly in LN years.
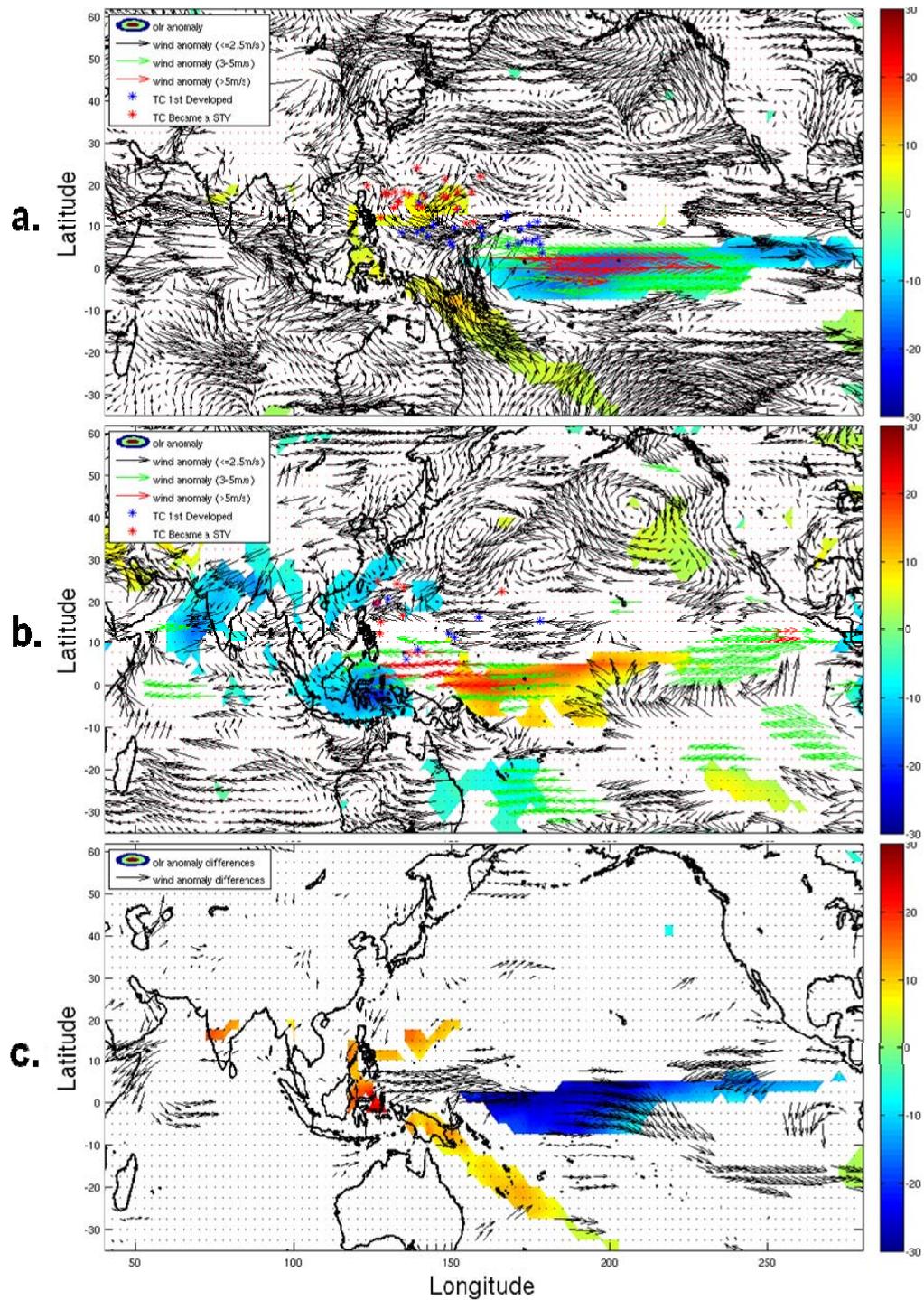
Figure 30.   As in Figure 28, except (a) positive ENSO and positive PDO years (5), (b) negative ENSO and negative PDO years (3), and (c) their difference. Blue markers identify TC formation locations of TCs that reached STY category. The red markers identify locations where the TCs achieved STY intensity.
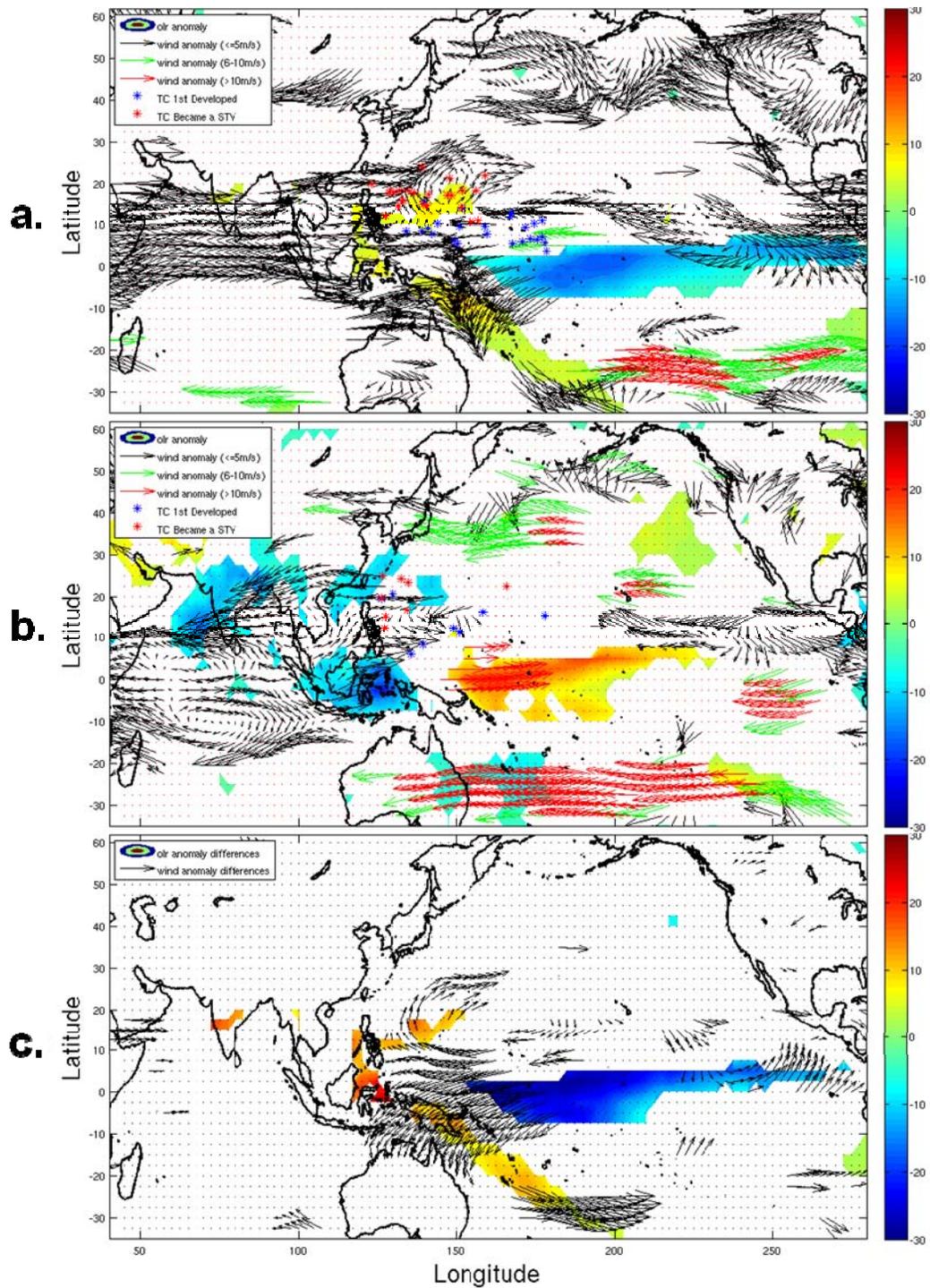
Figure 31.　As in Figure 30, except OLR (shaded, W/m^2) and 200-hPa winds (vectors, m/s). Blue markers identify TC formation locations of TCs that reached STY category. The red markers identify locations where the TCs achieved STY intensity.

Composites of low-level wind anomalies based on the combination of ENSO and AAO differ from those of ENSO only or ENSO and PDO as there are fewer significant vectors over the equatorial Pacific (Figure 32). Positive ENSO and negative AAO are associated with weaker westerly wind anomalies at the lower levels (Figure 32a), as well as less significant areas of positive and negative OLR. There is significant cross-equatorial flow from the Southern Hemisphere over the equatorial western Pacific as the AH is strong and shifts equatorward. Over the South Indian Ocean, the MH is stronger than normal, which is a characteristic associated with a negative AAO. During LN/AAO+ (Figure 32b), easterly anomalous across the equatorial Pacific are much reduced from ENSO and ENSO/PDO composites. Furthermore, significant cross-equatorial flow over the western Pacific is directed from the Northern Hemisphere. Therefore, during LN/AAO+ events, the MT over the WNP is weaker than normal, which is consistent with the low ACE values (Table 6). The significant differences between EN/AAO- and LN/AAO+ (Figure 32c) are linked to zonal winds across the central equatorial Pacific, which suggests that EN/LN differences dominate this combination rather than differences in phases of the AAO.

At upper levels (Figure 33), anomalies are dominated by zonal winds across equatorial latitudes and are similar to the ENSO and ENSO/PDO patterns. Differences between EN/AAO- and LN/AAO+ are also confined to the equatorial Pacific, which emphasizes the dominance of ENSO in these composites.
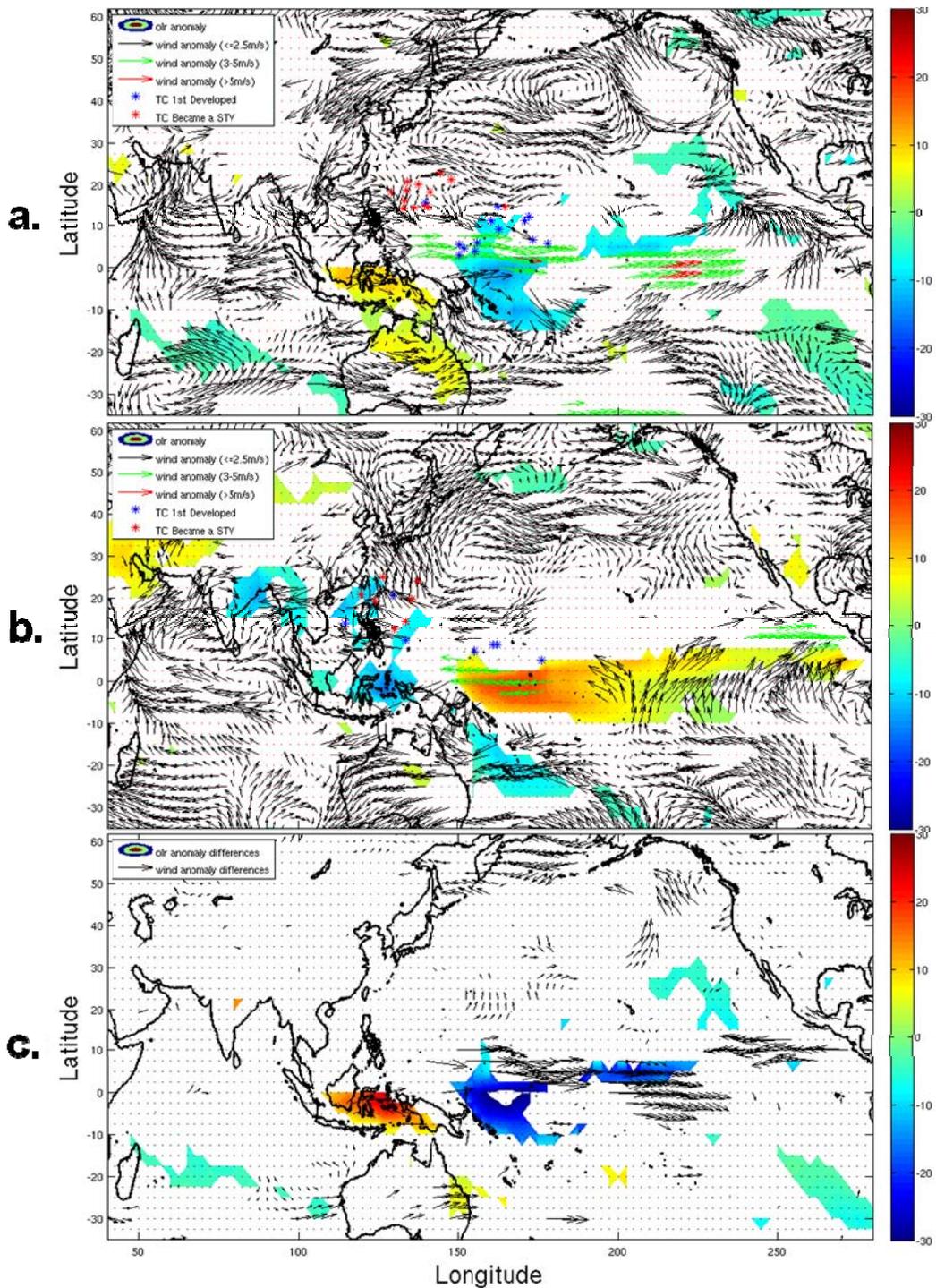
Figure 32.   As in Figure 28, except (a) positive ENSO and negative AAO years (3), (b) negative ENSO and positive AAO years (3), and (c) their difference. Blue markers identify TC formation locations of TCs that reached STY category. The red markers identify locations where the TCs achieved STY intensity.
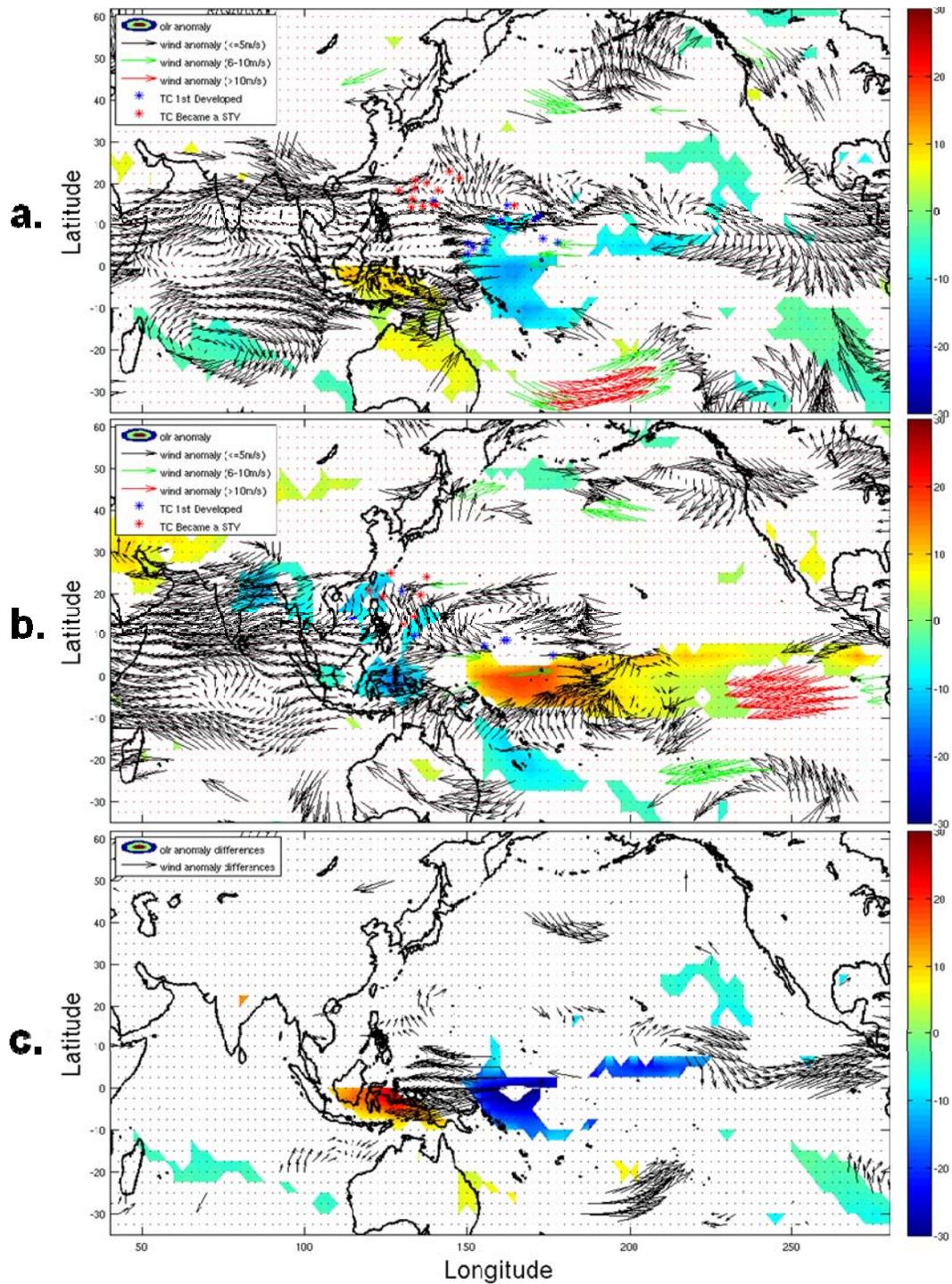
Figure 33.   As in Figure 32, except OLR (shaded, W/m^2) and 200-hPa winds (vectors, m/s). Blue markers identify TC formation locations of TCs that reached STY category. The red markers identify locations where the TCs achieved STY intensity.

Similar composites of the three-dimensional combinations of large-scale circulations were also examined to highlight the influence of all combinations working together on TC activity in the WNP. The only three-dimensional combination that was statistically significant was the ENSO/PDO/AAO combination (Table 6). At the 850-mb level, positive ENSO, positive PDO, and negative AAO conditions contained strong westerly anomalies over most of the equatorial central Pacific (Figure 34a). A strong cyclonic anomaly is present over the northeastern Pacific with a weaker cyclonic anomaly over the WNP. The anomalous cross-equatorial winds from the AH are quite strong, but positive OLRA (decreased deep convection) exists over the Maritime Continent, New Guinea, and the northeastern portion of Australia. Opposite conditions exist for the negative ENSO, negative PDO, and positive AAO combination (Figure 34b). Strong easterly wind anomalies and positive OLRA (decreased deep convection) are found over the equatorial central Pacific region. A strong anticyclonic anomaly exists over the northeastern Pacific, stronger anomalous cross-equatorial flow are in the Indian Ocean associated with the MH, and decreased cross-equatorial winds are in the WNP associated with the AH (Figure 34b). Again, the composite difference field indicates that significant anomalies are restricted to the equatorial Pacific, which defines the dominant ENSO signal in the composite (Figure 34c).

At the 200-hPa level (Figure 35), composites are dominated by zonal winds over the equatorial region of the Indian and Pacific Ocean, which are similar to the ENSO composites. The strong anticyclonic anomaly over the WNP during the combined positive ENSO, positive PDO, and negative AAO years (Figure 35a) tends to favor TC development. However, during the combined negative ENSO, negative PDO, and positive PDO years the opposite is true with a weak cyclonic anomaly over the WNP (Figure 35b). The only significant differences (Figure 35c) are over the equatorial western Pacific, which again relate to the dominance of the ENSO pattern on these combinations.

Finally, similar composites at 850-hPa and 200h-Pa levels (Figure 36 and 37) were examined for the four-dimensional combinations of large-scale circulations. Strong low-level westerly anomalies prevail over the entire equatorial central Pacific Ocean

54

during the positive four-dimensional composite, with strong cross-equatorial wind anomalies from the AH west of 170°E (Figure 36a). These low-level wind anomalies would tend to favor WNP TC development. During the negative phase of the four-dimensional combination, easterly wind anomalies are dominant over the equatorial central Pacific and significantly fewer cross-equatorial winds are coming into the WNP from the AH, which would not favor TC development in the WNP (Figure 36b). The much more pronounced anticyclone over the northeastern Pacific Ocean is now indicative of negative PDO and LN effects. The composite difference field (Figure 36c) has weak westerly wind anomalies over most of the equatorial central Pacific Ocean. At the 200-hPa level, easterly wind anomalies prevail during years with the positive four-dimensional combination (Figure 37a) and westerly wind anomalies during the negative combination (Figure 37b). An upper-level anticyclonic anomaly is dominant over the WNP during the positive four-dimensional phase, which favors TC development. This anticyclonic anomaly is also seen in the composite difference field (Figure 37c), as well as easterly wind anomalies over the western equatorial Pacific Ocean.
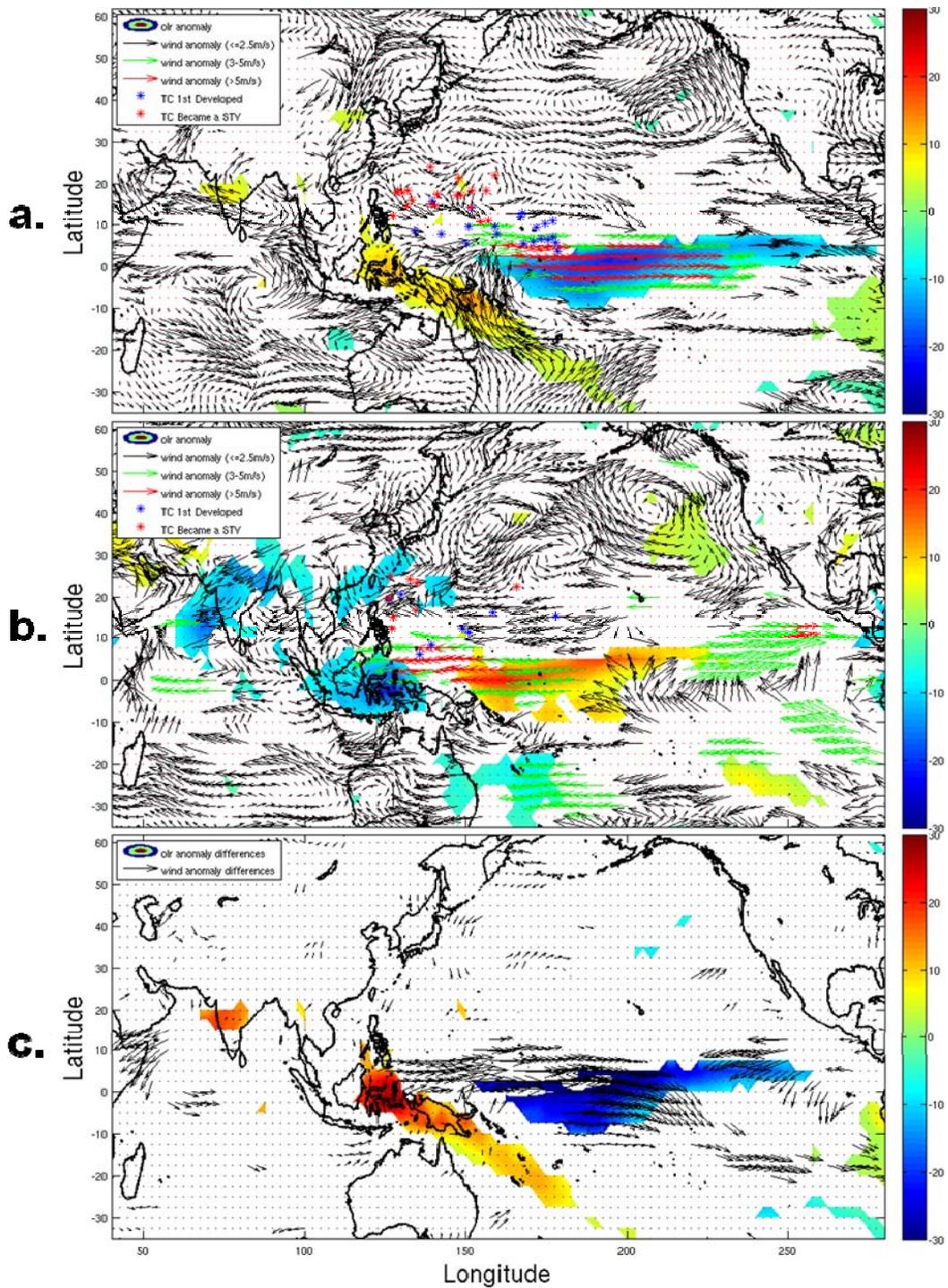
Figure 34.   As in Figure 28, except (a) positive ENSO, positive PDO, and negative AAO years (4), (b) negative ENSO, negative PDO, and positive AAO years (3), and (c) their difference. Blue markers identify TC formation locations of TCs that reached STY category. The red markers identify locations where the TCs achieved STY intensity.
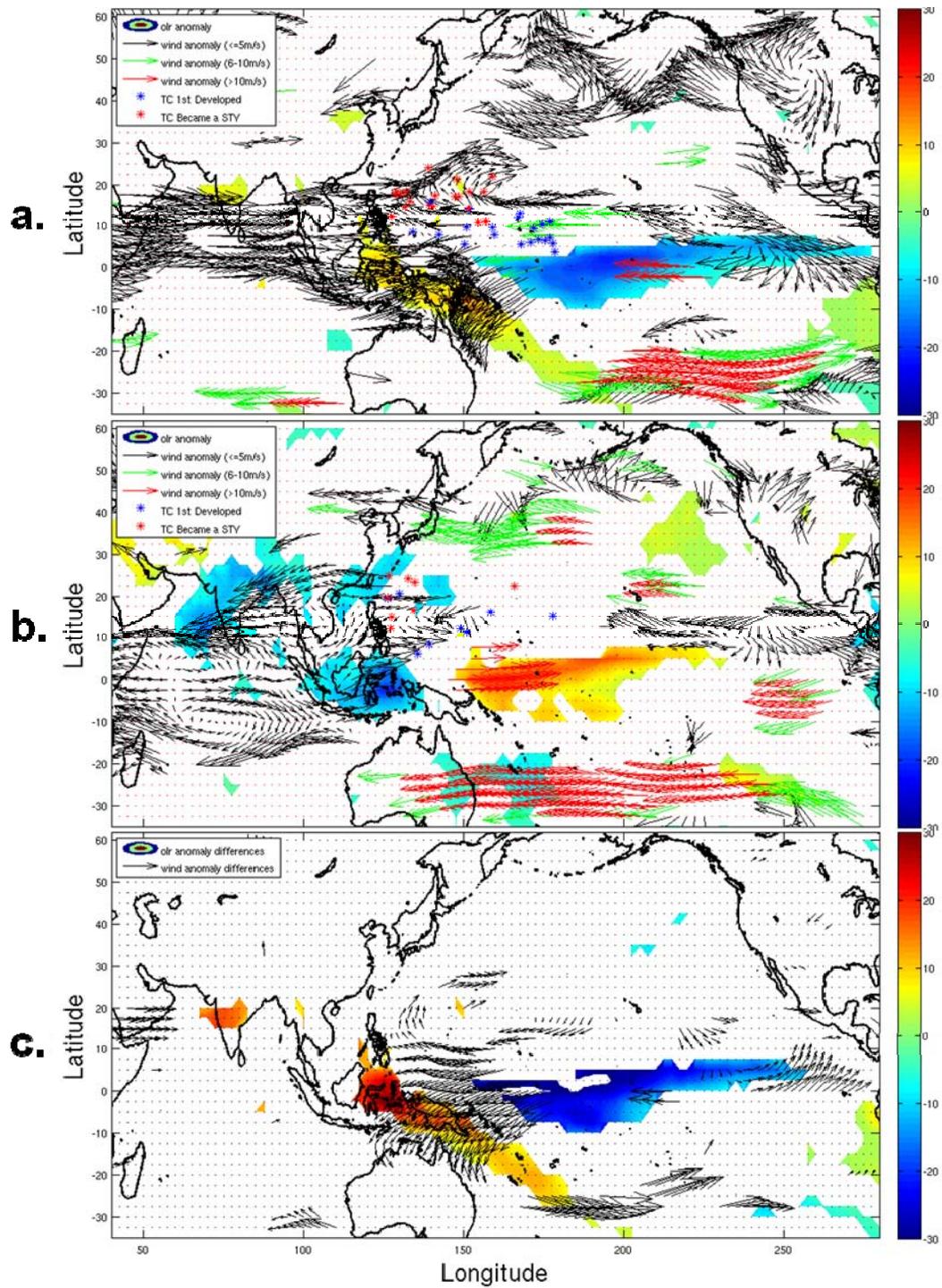
Figure 35.   As in Figure 34, except OLR (shaded, W/m^2) and 200-hPa winds (vectors, m/s). Blue markers identify TC formation locations of TCs that reached STY category. The red markers identify locations where the TCs achieved STY intensity.
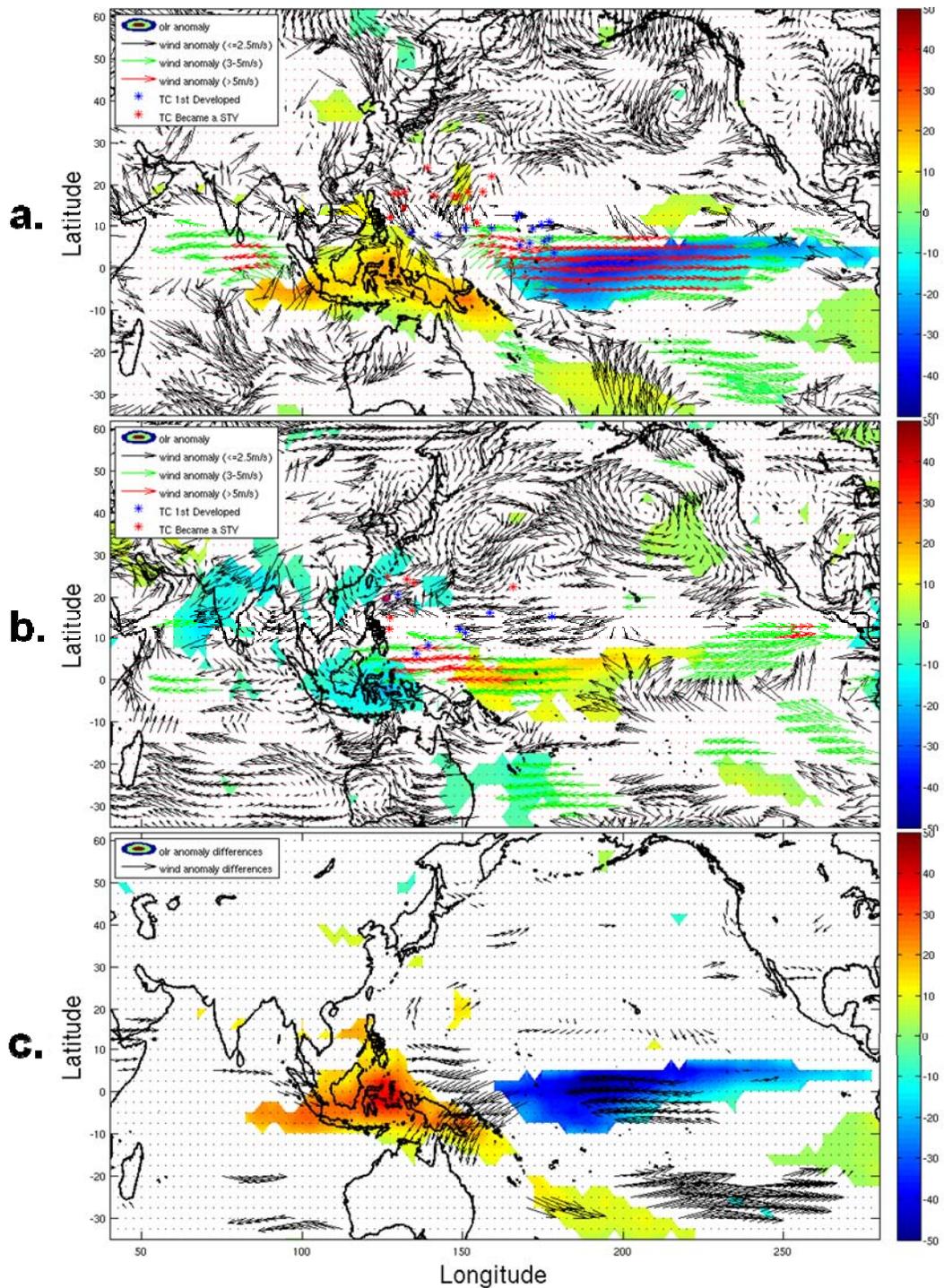
Figure 36.   As in Figure 28, except (a) positive ENSO, positive PDO, positive IOD, and
negative AAO years (2), (b) negative ENSO, negative PDO, negative IOD,
and positive AAO years (3), and (c) their difference. Blue markers identify
TC formation locations of TCs that reached STY category. The red markers
identify locations where the TCs achieved STY intensity.
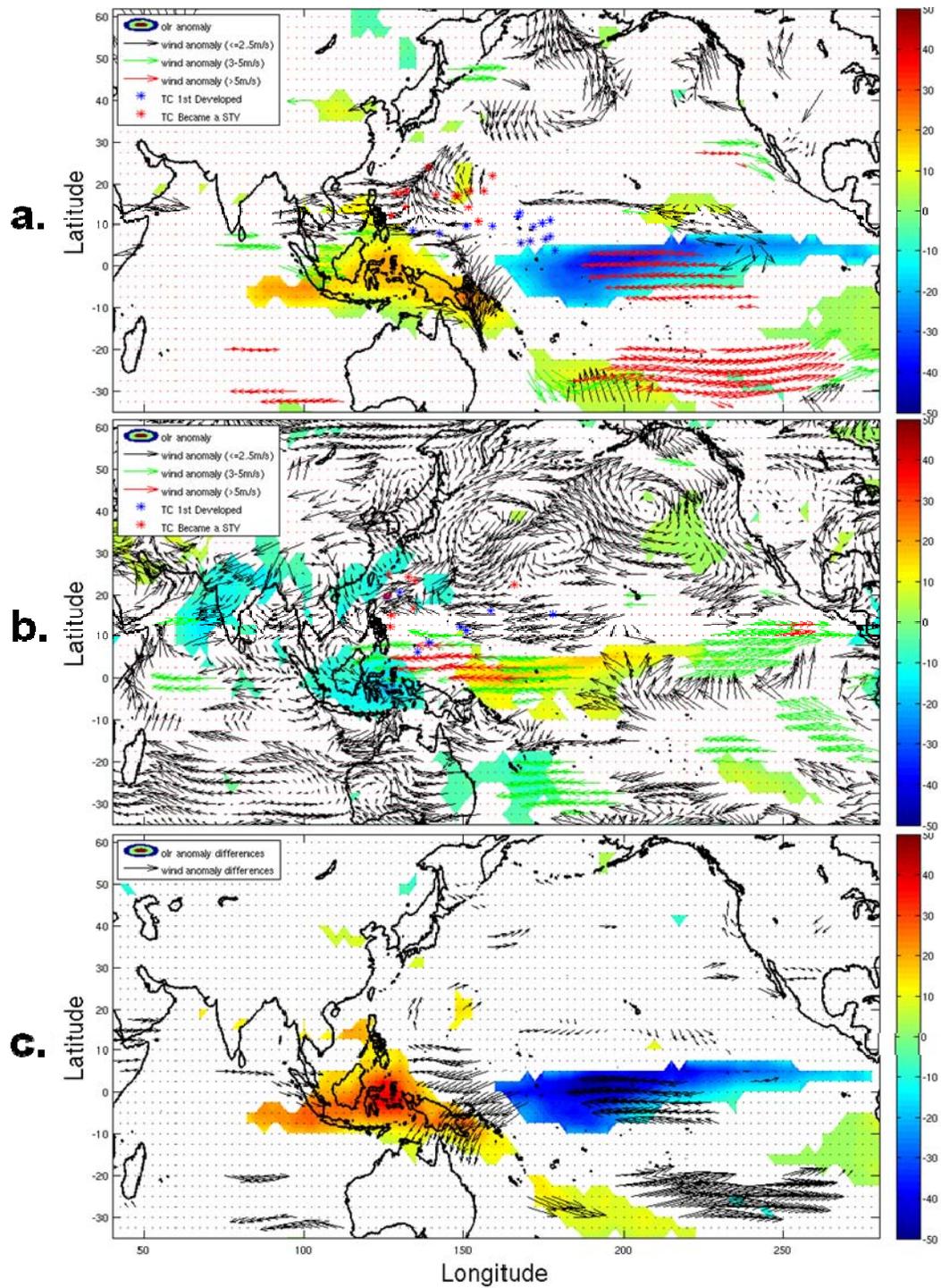
Figure 37.   As in Figure 36, except OLR (shaded, W/m^2) and 200-hPa winds (vectors, m/s). Blue markers identify TC formation locations of TCs that reached STY category. The red markers identify locations where the TCs achieved STY intensity.

THIS PAGE INTENTIONALLY LEFT BLANK

IV. CONCLUSION

A. SUMMARY

This thesis analyzed the anomalous large-scale circulations over the WNP during the 2008 TC season. Other seasons similar to 2008 were also analyzed to determine systematic characteristics associated with TC activity. The 2008 TC season started as active in May, but quickly became inactive through October. October was a record setting month in that no typhoons occurred, which is first in JTWC records. Strong easterly wind anomalies at the lower levels dominated most of the WNP. The easterly anomalies are indicative of a strongly negative PDO signal and a weak MT, which brought about LN-like conditions for the Pacific. Officially, the ENSO state was Neutral during the primary TC season, but became LN in November 2008. A strong tropical tropospheric upper trough (TUTT) and cells in the TUTT dominated the upper-level circulation over the WNP during 2008. A consecutive 3-year positive IOD (a rare event) also occurred. Other conditions present during 2008 included a positive AAO, which is also associated with LN-like conditions over the WNP, but was not found to be a major contributor to TC activity in the WNP.

This thesis also addressed how particular combinations of large-scale circulations influence TC activity in the WNP. Using statistical analysis and seasonal composites, it was established that large-scale circulations and MT climatology play a vital role in TC activity in a particular TC season. The basic hypothesis of this research was that TC formation occurs when the large-scale circulations provide the trigger and convection necessary for cyclogenesis. Statistical data, OLR seasonal composites, and upper- and lower-level wind fields were analyzed for general features that could be related with TC formation during specific large-scale circulation patterns and combinations.

Combinations of positive and negative phases of the circulation systems were examined when more than one year was contained in the combinations. The differences in ACE and STY values during combinations of positive and negative phases of each index were examined as described for years in which individual circulation phases

existed. For the two-dimensional combinations (Table 6) only differences between years that contained opposite phases of ENSO were statistically significant (i.e., [EN/PDO+, LN/PDO-], [EN/AAO-, LN/AAO+], [EN/MT+, LN/MT-]). Combinations of three circulation indices contained only two possible types and only one of the combinations (ENSO/PDO/AAO) was significant (Table 6). Only one combination of four circulations contained more than one year. The ACE values and number of STY during years with EN/PDO+/IOD+/AAO- were significantly different from years with LN/PDO-/IOD-/AAO+.

The results in Table 6 indicate that significant differences in ACE only occur during years in which ENSO has opposite phases. Differences in ACE values and numbers of STYs during years of opposite phase for other circulation indices do not exhibit significant differences. This was also found for years of combinations of indices. Only combinations that included opposite phases of ENSO have a significant impact on TC activity over the WNP.

Statistical and composite analyses demonstrate strong occurrences and intensity relationships between TC activity and large-scale circulations, not only in the regional sense, but also in the global sense. As has been documented by many other authors, the relationship between ENSO and storm numbers is clear. In this thesis, the relationships are further analyzed by incorporating additional effects of other large-scale circulations in the WNP region. It was established that the strongest mode of interannual variability in storm activity is one in which the ENSO is involved, whether by itself or in combinations with other signals. Other large-scale circulations tend to intensify the effects of an existing ENSO signal by increasing westerly and/or easterly wind anomalies, intensifying cyclonic and/or anticyclonic anomalies in the region, intensifying or decreasing cross-equatorial winds, influencing SST anomalies, etc. The PDO has the second largest influence after ENSO, followed by MT and AAO, and to a lesser degree IOD. Individually, these other circulations are non-significant, but in combination with the ENSO may have important effects on TC activity. That is, PDO, MT, AAO, and IOD reinforce ENSO signal on different levels.

B.   FUTURE STUDY

Future studies could exploit the use of PDO and lesser signals in long-range forecast schemes and TC activity predictions. Larger samples may lead to some of the large-scale circulations other than ENSO becoming statistically significant, especially where the differences between phases are almost significant. Then these smaller signals and their influence can also be incorporated in future TC forecasting schemes.

THIS PAGE INTENTIONALLY LEFT BLANK

LIST OF REFERENCES

Bell, G. D., M. S. Halpert, R. C. Schnell, R. W. Higgins, J. Lawrimore, V. E. Kousky, R. Tinker, W. Thiaw, M. Chelliah, and A. Artusa, 2000: Climate assessment for 1999. *Bull. Amer. Meteor. Soc.,* **81**, s1-s50.

Briegel, L. M., and W. M. Frank, 1997: Large-scale influences on tropical cyclogenesis in the western North Pacific. *Mon. Wea. Rev.,* **125**, 1397-1413.

Burton, K. R., (U.S.), 2005: Influence of Antarctic oscillation on intraseasonal variability of large-scale circulations over the western North Pacific. M.S. thesis. Naval Postgraduate School. [electronic resource]. 93. 2-15.

Chan, J. C. L., J. Shi, and K. S. Liu, 2001: Improvements in the seasonal forecasting of tropical cyclone activity over the western North Pacific. *Wea. and Forecasting,* **16**, 491-498.

Camargo, S. J., 2009: Tropical cyclones, western North Pacific basin, in State of the Climate in 2008. *To appear in Bull. Amer. Meteor. Soc.,* July 2009.

Camargo, S. J., and A. H. Sobel, 2005: Western North Pacific tropical cyclone intensity and ENSO. *J. Climate,* **18**, 2996-3006.

Camargo, S. J., K. A. Emanuel, and A. H. Sobel, 2007a: Use of a genesis potential index to diagnose ENSO effects on tropical cyclone genesis. *J. Climate,* **20**, 4819-4834.

Camargo, S. J., A. W. Robertson, S. J. Gaffney, P. Smyth, and M. Ghil, 2007b: Cluster analysis of typhoon tracks. Part I: General properties. *J. Climate,* **20**, 3635-3653.

Camargo, S. J., A. W. Robertson, S. J. Gaffney, P. Smyth, and M. Ghil, 2007: Cluster analysis of typhoon tracks. Part II: Large-scale circulation and ENSO. *J. Climate,* **20**, 3654-3676.

Carvalho, L. M. V., C. Jones, and T. Ambrizzi, 2005: Opposite phases of the Antarctic Oscillation and relationships with intraseasonal to interannual activity in the tropics during the austral summer. *J. Climate,* **18**, 702-718.

Chan, J. C. L., 2008: Decadal variations of intense typhoon occurrence in the western North Pacific. *Proceedings of the Royal Society A: Mathematical, Physical and Engineering Sciences,* **464**, 249-272.

Chan, J. C. L., J. Shi, and C. Lam, 1998: Seasonal forecasting of tropical cyclone activity over the western North Pacific and the South China Sea. *Wea. and Forecasting,* **13**, 997-1004.

Delk, T. L., (U.S.), 2004: Intraseasonal, large-scale circulations and tropical cyclone activity over the Western North Pacific during Boreal summer. M.S. thesis. Naval Postgraduate School. [electronic resource]. 77. 1-17.

Dretzke, B. J., 2001: *Statistics with Microsoft Excel.* Second Edition. Prentice Hall, 257 pp.

Fogt, R. L., and D. H. Bromwich, 2006: Decadal variability of the ENSO teleconnection to the high-latitude South Pacific governed by coupling with the Southern Annular Mode*. *J. Climate,* **19**, 979-997.

Frank, W. M., and P. E. Roundy, 2006: The role of tropical waves in tropical cyclogenesis. *Mon. Wea. Rev.,* **134**, 2397-2417.

Gershunov, A., and T. P. Barnett, 1998: ENSO influence on intraseasonal extreme rainfall and temperature frequencies in the contiguous United States: Observations and model results. *J. Climate,* **11**, 1575-1586.

Gershunov, A., and T. P. Barnett, 1998: Interdecadal modulation of ENSO teleconnections. *Bull. Amer. Meteor. Soc.,* **79**, 2715-2725.

Gershunov, A., T. P. Barnett, and D. R. Cayan, 1999: North Pacific interdecadal oscillation seen as factor in ENSO-related North American climate anomalies. *EOS,* **80**, 25-30, 1999.

Gershunov, A., T. P. Barnett, D. R. Cayan, T. Tubbs, and L. Goddard, 2000: Predicting and downscaling ENSO impacts on intraseasonal precipitation statistics in California: The 1997/98 Event. *J. Hydrometeor.,* **1**, 201-210.

Gong, D., and S. Wang, 1999: Definition of Antarctic Oscillation Index. *Geophys. Res. Lett.,* **26**, 459-462, 1999.

Gray, W. M., 1968: Global view of the origin of tropical disturbances and storms. *Mon. Wea. Rev.,* **96**, 669-700.

Harr, P. A., and R. L. Elsberry, 1991: Tropical cyclone track characteristics as a function of large-scale circulation anomalies. *Mon. Wea. Rev.,* **119**, 1448-1468.

Lander, M. A., 1996: Specific tropical cyclone track types and unusual tropical cyclone motions associated with a reverse-oriented monsoon trough in the western North Pacific. *Weather and Forecasting,* **11**, 170-186.

Lander, M. A., and C. P. Guard, 1998: A look at global tropical cyclone activity during 1995: Contrasting high Atlantic activity with low activity in other basins. *Mon. Wea. Rev.,* **126**, 1163-1173.

Mantua, N. J., 1999: The Pacific Decadal Oscillation and Climate Forecasting for North America. *Joint Institute for the Study of the Atmosphere and Oceans University of Washington, Seattle, Washington, USA.*

Mantua, N. J., S. R. Hare, Y. Zhang, J. M. Wallace, and R. C. Francis, 1997: A Pacific interdecadal climate oscillation with impacts on salmon production. *Bull. Amer. Meteor. Soc.,* **78**, 1069-1079.

McCabe, G. J., M. D. Dettinger, 1999: Decadal variations in the strength of ENSO teleconnections with precipitation in the western United States. *Intern. J. Clima.,* **19**, 1399-1410, 1999.

McCabe, G. J., and M. D. Dettinger, 2002: Primary modes and predictability of year-to-year snowpack variations in the western United States from teleconnections with Pacific Ocean climate. *J. Hydrometeor.,* **3**, 13-25.

Minobe, S., 1997: A 50-70 year climatic oscillation over the North Pacific and North America. *Geophys. Res. Lett.,* **24**, 683-686, 1997.

Murphree, T., 2008: Indian Ocean Zonal Mode Module, Modern Climatology, MR 3610, class. Naval Postgraduate School*, 2008.*

Rasmusson, E. M., and T. H. Carpenter, 1982: Variations in tropical sea surface temperature and surface wind fields associated with the Southern Oscillation/El Niño. *Mon. Wea. Rev.,* **110**, 354-384.

Saji, N. H., B. N. Goswami, P. N. Vinayachandran, and T. Yamagata, 1999: A dipole mode in the tropical Indian Ocean. *Nature,* **401**, 360-363, 1999.

Sasaki, K., 2009: *Summary of the 2008 Typhoon Season. RMSC Tokyo*, WRD/TC.41/6 Add. 1.

Shinoda, T., and W. Han, 2005: Influence of the Indian Ocean Dipole on atmospheric subseasonal variability. *J. Climate,* **18**, 3891-3909.

Thompson, D. W. J., and D. J. Lorenz, 2004: The signature of the annular modes in the tropical troposphere. *J. Climate,* **17**, 4330-4342.

Thompson, D. W. J., and S. Solomon, 2002: Interpretation of recent Southern Hemisphere climate change. *Science,* **296**, 895-899.

Thompson, D. W. J., and J. M. Wallace, 2000: Annular modes in the extratropical circulation. Part I: Month-to-month variability. *J. Climate,* **13**, 1000-1016.

Trenberth, K.E., and J.W. Hurrell, 1994: Decadal atmosphere-ocean variations in the Pacific. *Climate Dynamics,* **9**, 303-303.

Trenberth, K. E., 1990: Recent observed interdecadal climate changes in the Northern Hemisphere. *Bull. Amer. Meteor. Soc.,* **71**, 988-993.

Wang, B., 2006: *The Asian Monsoon.* Springer, 787 pages.

Wang, B., and J. C. L. Chan, 2002: How strong ENSO events affect tropical storm activity over the western North Pacific. *J. Climate,* **15**, 1643-1658.

Xu, J., and J. C. L. Chan, 2001: The role of the Asian–Australian monsoon system in the onset time of El Niño events. *J. Climate,* **14**, 418-433.

Xue, F., H. Wang, and J. He, 2004: Interannual variability of Mascarene high and Australian high and their influences on east Asian summer monsoon. *J. Meteor. Soc. Japan,* **82**, 1173-1186, 2004.

Zhang, Y., J. M. Wallace, and D. S. Battisti, 1997: ENSO-like interdecadal variability: 1900–93. *Journal of Climate,* **10**, 1004-1020.

INITIAL DISTRIBUTION LIST

1. Defense Technical Information Center
    Ft. Belvoir, Virginia

2. Dudley Knox Library
    Naval Postgraduate School
    Monterey, California

3. Professor Philip Durkee
    Naval Postgraduate School
    Monterey, California

4. Professor Russell Elsberry
    Naval Postgraduate School
    Monterey, California

5. Professor Patrick Harr
    Naval Postgraduate School
    Monterey, California

6. Director, Joint Typhoon Warning Center
    Naval Pacific Meteorology and Oceanography Center
    Pearl Harbor, Hawaii

7. Lieutenant Commander Ricardo Trevino
    PSC 831 CJTF-HOA
    J3 METOC
    FPO, AE